

## Band-theoretic calculations of the optical-activity tensor of $\alpha$ -quartz and trigonal Se

Hua Zhong\* and Zachary H. Levine

*Department of Physics, The Ohio State University, Columbus, Ohio 43210-1368*

Douglas C. Allan

*Materials Research Department, SP-PR-22, Corning Incorporated, Corning, New York 14831  
and Department of Physics, The Ohio State University, Columbus, Ohio 43210-1368*

John W. Wilkins

*Department of Physics, The Ohio State University, Columbus, Ohio 43210-1368*

(Received 7 January 1993)

We present a formalism to compute the optical-activity tensor in the long-wavelength limit neglecting local-field corrections with a nearly first-principles approach. The calculation of optical activity requires perturbation theory in the vector potential in order to describe the rotation of the plane of polarization perpendicular to the direction of propagation. We contrast this approach with perturbation theory in the scalar potential which can be used for the other optical response properties we compute. Band structures are obtained within the Kohn-Sham local-density approximation using standard plane-wave and separable norm-conserving pseudopotential techniques. Self-energy effects necessary to obtain the correct band gap are included by the use of a "scissors operator." In the long-wavelength limit, two components of the optical-activity tensor are computed for both selenium and  $\alpha$ -quartz. For selenium in the low-frequency range, the optical rotatory power along the optic axis is about a factor of 2 too small compared with some of the experimental data. For  $\alpha$ -quartz, the ratio  $g_{11}/g_{33}$  and the frequency dependence of both components obey the phenomenological coupled-oscillator model and are in agreement with experiment. Yet both  $g_{11}$  and  $g_{33}$  (or the optical rotatory power) are about a factor of 5 too small compared with the available experimental data. In addition, the dielectric constants and second-harmonic-generation susceptibilities including local-field corrections are calculated for selenium and  $\alpha$ -quartz in terms of scalar-potential theory. Excellent agreement (discrepancies of a few percent) is obtained with the experiments for these properties.

### I. INTRODUCTION

In a previous paper,<sup>1</sup> we presented a calculation of the optical-activity tensor of trigonal selenium with a nearly first-principles approach. The purpose of this paper is to give a detailed derivation of the formalism and to expand and correct our presentation of the calculations. We also report our study of the optical response functions of  $\alpha$ -quartz.

Optical rotation describes the ability of a medium to rotate the plane of polarization of linearly polarized light that is transmitted through it. This effect was discovered by Arago (1811) by propagating linearly polarized sunlight along the optic axis of quartz.<sup>2</sup> This observation attracted a great deal of attention in the development of 19th century optics including work by such notable figures as Airy (1836), Cauchy (1850), Clebsch (1859), Lommel (1881),<sup>3</sup> and Drude (1892),<sup>4</sup> and led to the development of stereochemistry. Optical activity was first explained by Biot (1812) and Fresnel (1816).<sup>2</sup> They found that linearly polarized light can be decomposed into two circular polarizations with opposite handedness. In an optically active material the two circularly polarized light waves constitute normal modes and travel with different velocities. After passing through the optically active material, the two circularly polarized light waves recombine

and produce a linearly polarized wave with the plane of the polarization rotated with respect to the original direction of the linear polarization. This optical rotation is the most well-known phenomenon in optical activity. The rotation of the plane of polarization is quantitatively described by the rotation angle per unit length, which is defined as optical rotatory power  $\rho$ . It is related to the refractive indices for left ( $n_L$ ) and right ( $n_R$ ) circularly polarized light by

$$\rho = \frac{\omega}{2c} (n_L - n_R). \quad (1.1)$$

In past work sign conventions have not been unambiguous. We take our conventions from a careful analysis by Glazer and Stadnicka.<sup>5</sup>

There has been some success in making phenomenological models and quantum-mechanical theories of this phenomenon (see Ref. 6 for a review), one of the simplest of which is a coupled-oscillator model which can be treated either classically or quantum mechanically.<sup>7</sup> A rigorous quantum-mechanical treatment including numerical predictions has been missing, the needed expressions being considered "difficult if not impossible to calculate numerically."<sup>4</sup> The present paper pursues that goal.

One form of the coupled-oscillator model<sup>8,9</sup> yields a

dispersion relation for optical rotatory power of

$$\rho(\omega) = \frac{k\omega^2}{(\omega^2 - \omega_0^2)^2}, \quad (1.2)$$

where  $k$  and  $\omega_0$  are parameters. Analysis of the experimental data on various optically active crystals shows<sup>4</sup> that Eq. (1.2) is a general dispersion relation for the optical rotatory power in the subband-gap regime. The coupled-oscillator model is analogous to the single-effective-oscillator model<sup>10</sup> (which has the same form as a one-term Sellmeier equation<sup>11</sup>), which is successful in describing the dielectric function of semiconductors and insulators. More recently, a semiempirical model,<sup>5,12</sup> which assumes that the response of a crystal to an electromagnetic field is a superposition of the responses from individual atoms in the crystal, has been applied to quantitatively calculate the optical rotatory power. The polarizabilities of the atoms are treated as parameters to be adjusted to fit the experimental data. Such an approach yields a considerable variation in polarizability of a given atom in different crystals and as a result has limited predictive power.

There have been considerable theoretical and computational advances in band-theoretic optical response calculations.<sup>13–18</sup> With the inclusion of the self-energy effects, the modified time-dependent local-density approximation has been used to study the dielectric constants,<sup>19,20</sup> second-harmonic susceptibilities,<sup>21,22</sup> and the photoelastic tensor<sup>23</sup> with success. In this paper we extend this approach to the study of optical activity. The organization of the paper is as follows. Section II contains a brief review of the classical theory of optical activity, wherein the characteristic quantities for optical activity are defined. The detailed derivation of the optical activity tensor for a periodic system from one-electron perturbation theory is presented in Sec. III. Section IV reports the computed results of the optical response functions, including the dielectric function, second-harmonic susceptibilities, optical rotatory power, and the gyration tensor component  $g_{11}$  of trigonal selenium and  $\alpha$ -quartz. Section V is a summary. A more complete discussion of this work may be found in Ref. 24.

## II. CLASSICAL THEORY OF OPTICAL ACTIVITY

A system is called “optically active” if it has different response to right and left circularly polarized light. Mathematically, optical activity is defined through the constitutive relation

$$D_i = \epsilon_{ij}E_j + \eta_{ijl}\nabla_j E_l, \quad (2.1)$$

where we adopt notation from Ref. 4 for the optical activity tensor  $\eta_{ijl}$ . The Einstein summation convention is used in this paper. Equation (2.1) is a generalization of the common constitutive relation  $D_i = \epsilon_{ij}E_j$  and can be considered to be a Taylor expansion to first order in the derivative of  $\mathbf{E}$ , or first order in  $\mathbf{B}$ . In other words, optical activity results from the spatial dispersion of the dielectric response. In general<sup>25</sup>  $\eta_{ijl}$  is antisymmetric in the first and third indices, i.e.,

$$\eta_{ijl} = -\eta_{lji}, \quad (2.2)$$

so that only 9 of the 27 components in the third-rank tensor  $\eta_{ijl}$  are independent. In the absence of absorption these components must be real.<sup>25</sup>

The 9 independent components of  $\eta_{ijl}$  may be rewritten in terms of the gyration tensor  $g_{ij}$ , which is also commonly used to describe optical activity.<sup>26–28</sup> (Others define  $g_{ij}$  differently.<sup>4,25</sup>) The gyration tensor is related to the optical activity tensor  $\eta_{ijl}$  by

$$g_{mj} = \frac{1}{2}q e_{iml} \eta_{ijl}, \quad (2.3)$$

where  $e_{iml}$  is the completely antisymmetric unit tensor and  $q$  is the magnitude of the wave vector. Crystal symmetry restricts the form of  $g_{ij}$ .<sup>27</sup> For example, crystals with 32 point group symmetry (to which both trigonal selenium and  $\alpha$ -quartz belong) are uniaxial with the optic axis along the  $c$  axis (defined as the  $z$  axis) and the gyration tensor is of the form

$$\begin{pmatrix} g_{11} & 0 & 0 \\ 0 & g_{11} & 0 \\ 0 & 0 & g_{33} \end{pmatrix}. \quad (2.4)$$

The relation between the gyration tensor and optical rotatory power  $\rho$  can be obtained from the wave equation. In nonmagnetic semiconductors, the Maxwell equations can be written as

$$\mathbf{B} = \mathbf{H}, \quad (2.5)$$

$$\nabla \times \mathbf{B} = \frac{1}{c} \frac{\partial \mathbf{D}}{\partial t} = \frac{1}{c} \frac{\partial \mathbf{E}}{\partial t} + \frac{4\pi}{c} \mathbf{J}. \quad (2.6)$$

In the  $\phi=0$  gauge, the fields are related to the vector potential by the relations

$$\mathbf{E} = -\frac{1}{c} \frac{\partial \mathbf{A}}{\partial t} \quad (2.7)$$

and

$$\mathbf{B} = \nabla \times \mathbf{A}. \quad (2.8)$$

Equations (2.5)–(2.8) lead to the wave equation

$$\nabla^2 \mathbf{A} - \frac{1}{c^2} \frac{\partial^2 \mathbf{A}}{\partial t^2} - \nabla(\nabla \cdot \mathbf{A}) = -\frac{4\pi}{c} \mathbf{J}, \quad (2.9)$$

where the induced current  $\mathbf{J}$  can be written in terms of the dielectric matrix and optical-activity tensor with the use of the constitutive equation, Eq. (2.1), and the monochromatic assumption  $\mathbf{A}(\mathbf{r}, t) = \mathbf{A}_q e^{i(\mathbf{q} \cdot \mathbf{r} - \omega t)}$ ,

$$\begin{aligned} \hat{\mathbf{i}} \cdot \mathbf{J}_q &= -\frac{i\omega}{4\pi} \hat{\mathbf{i}} \cdot (\mathbf{D} - \mathbf{E}) \\ &= \frac{\omega^2}{4\pi c} (\epsilon_{ij} - \delta_{ij}) \hat{\mathbf{j}} \cdot \mathbf{A}_q + \frac{i\omega^2}{4\pi c} \eta_{ijl} q_j \hat{\mathbf{l}} \cdot \mathbf{A}_q. \end{aligned} \quad (2.10)$$

The wave equation, Eq. (2.9), and Eq. (2.10) yield the well-known “Fresnel’s equation of wave normals.”<sup>26</sup> In the absence of the linear birefringence,

$$\rho = \frac{\omega G}{2\pi c}, \quad (2.11)$$

where  $G \equiv g_{ij}l_i l_j$ ;  $(l_x, l_y, l_z)$  are the direction cosines of the wave vector  $\mathbf{q}$ , and  $\bar{n}$  is the mean refractive index for the direction of propagation. Using Eqs. (2.3) and (2.11) we find, for crystals belonging to the 32 point group, the optical rotatory power along the optic axis depends on the gyration component  $g_{33}$  (or  $\eta_{231}$ ) by the relation

$$\rho(\omega) = \frac{\omega}{2n_o c} g_{33} = \frac{\omega^2}{2c^2} \eta_{231}, \quad (2.12)$$

where  $n_o$  is the refractive index of the ordinary ray (which has its electric field in the basal plane).

Since  $G$  is small, optical activity can be considered as a perturbation on the linear birefringence<sup>27</sup> except for propagation along the optic axis where linear birefringence vanishes. The difference of the refractive indices  $n_o$  and  $n_e$  for linear birefringence is of order  $10^{-1} - 10^{-3}$  while the difference between  $n_L$  and  $n_R$  of optical activity is of order  $10^{-4} - 10^{-8}$ .<sup>29</sup> For this reason, observations of the optical rotation in a direction other than along the optic axis are few.<sup>28,30-32</sup> If the direction of the propagation is not in the direction of the optic axis, the solutions for the wave equation are two elliptically polarized waves.<sup>26</sup>

We have reviewed the basic macroscopic theory of the optical activity. In the next section we study the microscopic aspects of optical activity theory.

### III. ONE-ELECTRON BAND-THEORETIC FORMULA FOR THE OPTICAL ACTIVITY TENSOR

#### A. Introduction

As mentioned earlier, microscopic prediction of the optical activity of crystals is still limited to semiempirical models,<sup>5,6,4,9,12,33</sup> while the nearly first-principles one-electron band-theoretic approach has been applied to calculate the dielectric constants,<sup>19,20</sup> second-harmonic susceptibilities,<sup>21,22</sup> and the photoelastic tensor<sup>23</sup> with success. The one-electron approach based on the time-dependent local-density approximation has been presented elsewhere.<sup>20,34</sup>

In crystalline semiconductors and insulators, optical response calculations from the Kohn-Sham local-density approximation<sup>35</sup> (LDA) inevitably encounter the famous band-gap problem. The underestimation of the LDA gap causes an overestimation of the dielectric function. To solve the band-gap problem, the quasiparticle  $GW$  approximation<sup>36</sup> has been implemented.<sup>14,37</sup> It was found that the  $GW$  band gaps are accurate within about 0.1 eV of the experimental values; comparing the  $GW$  quasiparticle energies and the LDA eigenenergies for the systems investigated, the LDA eigenvalues can be corrected by an almost rigid shift on the conduction band for many materials. Moreover, the LDA wave functions are in almost perfect agreement with the  $GW$  quasiparticle wave functions.

However, if one naively switched from the LDA eigenvalues to the quasiparticle eigenenergies in optical response calculations, the calculated dielectric function, when compared with the experiments, would go from too large to too small. Levine and Allan<sup>19,20</sup> proposed a new

effective Hamiltonian

$$\hat{H}_k = \hat{H}_k^L + \hat{\Sigma}_k, \quad (3.1)$$

in which  $\hat{H}_k^L$  is the LDA Hamiltonian and the self-energy correction is approximated by the "scissors operator"  $\hat{\Sigma}_k = \Delta_k P_{ck}$ , where  $P_{ck}$  is a projection operator onto conduction-band states. The effect of the scissors operator is to shift the conduction bands upward by  $\Delta_k$  without changing the wave functions. This simple correction goes outside of density-functional theory to incorporate an approximation to the electron self-energy as revealed in  $GW$  calculations. In practice,  $\Delta_k$  has been replaced by a  $\mathbf{k}$ -independent parameter  $\Delta$ , which is determined from the  $GW$  approximation if available or from the experimental band gap. Due to the introduction of the self-energy, the velocity operator in the  $\mathbf{k} \cdot \mathbf{p}$  perturbation theory also needs<sup>19,20</sup> to be renormalized, i.e., the replacement  $\hat{\mathbf{p}} \rightarrow \hat{\mathbf{p}} + \nabla_{\mathbf{k}}(\Delta_k P_{ck})$  is required in perturbation theory. This approach has proved to be very effective in optical response calculations in various crystals.<sup>1,19-23</sup>

Most of the optical response functions are derived in terms of scalar-potential perturbation theory for real systems.<sup>13,14,19-22</sup> In scalar-potential perturbation theory, the polarization of the field is assumed to be parallel to the wave vector, i.e., only the longitudinal part of the field is considered. Therefore, scalar-potential perturbation theory is not suitable to describe the optical responses in which the directions of both the polarization and the wave vector of the field are important. The applicability of scalar-potential perturbation theory to calculate the dielectric constants in the long-wavelength limit can be understood through the arguments of Ambegaokar and Kohn.<sup>38</sup> With a general many-body physics argument, they proved that in a cubic system, the response to a long-wavelength electromagnetic field can be described by a single dielectric constant regardless of the polarization of the field when local-field corrections are neglected. (As far as we know, there is no theory on the compatibility of scalar- and vector-potential perturbation theories to calculate the dielectric constants when local fields are included.)

To describe optical activity, one needs to use a vector potential to describe the field so that the direction of the polarization and the wave vector can be distinguished. In vector-potential perturbation theory (in the  $\phi=0$  gauge) the perturbing electromagnetic field is represented by the vector potential  $\mathbf{A}$  and the response of the system is written in terms of the induced current density  $\mathbf{J}$ , whereas in the scalar-potential perturbation theory the external field is represented by  $\phi$  and the response by the induced charge density  $\rho$ .

#### B. Formulas

The first-order correction to the Hamiltonian which describes the interaction of an electromagnetic field with a system can be written in general<sup>39</sup> by

$$\hat{H}^{(1)}(t) = -\alpha \int d\mathbf{r} \hat{J}^{(0)}(\mathbf{r}) \cdot \mathbf{A}(\mathbf{r}, t), \quad (3.2)$$

where the superscript indicates the order of  $\mathbf{A}(\mathbf{r}, t)$ , which is the electromagnetic field in terms of a vector po-

tential and can be assumed to be in a monochromatic form

$$\mathbf{A}(\mathbf{r}, t) = \mathbf{A}_q e^{i(\mathbf{q}\cdot\mathbf{r} - \omega t)} = \mathbf{A}(\mathbf{r}) e^{-i\omega t}. \quad (3.3)$$

Atomic units are used hereafter; note that  $1/c \rightarrow \alpha = e^2/(\hbar c)$  in atomic units. In Eq. (3.2),  $\hat{\mathcal{J}}^{(0)}(\mathbf{r})$  is the unperturbed charge current operator at position  $\mathbf{r}$ , which is related to the velocity operator  $\hat{v}^{(0)} \equiv (-i)[\hat{p}, \hat{H}]$  as shown in Eq. (A3). Equation (3.2) is a generalization, which is still valid when a nonlocal potential is present, of the commonly used expression  $(\alpha/2)(\hat{\mathbf{p}} \cdot \mathbf{A} + \mathbf{A} \cdot \hat{\mathbf{p}})$ , which is still valid when a nonlocal potential is present. A detailed derivation of the perturbed Hamiltonian for a system with a nonlocal potential under the influence of an electromagnetic field can be found in Appendix A. The nonlocal potentials in our calculation are (1) the nonlocal pseudopotential,<sup>40</sup> which is introduced to replace the effects of the core electrons in the band-structure calculation, and (2) the self-energy  $\Sigma_{\mathbf{k}}$ , introduced through the scissors operator.

For a periodic system, the wave function can be written as

$$\langle \mathbf{r} | \psi_{n\mathbf{k}} \rangle = (N\Omega_0)^{1/2} e^{i\mathbf{k}\cdot\mathbf{r}} \langle \mathbf{r} | n\mathbf{k} \rangle, \quad (3.4)$$

where  $N$  is the number of unit cells,  $\Omega_0$  is the volume of the unit cell,  $n$  is the band index, and  $\mathbf{k}$  is the Bloch wave vector. The unperturbed Hamiltonian which operates on state  $|n\mathbf{k}\rangle$  is

$$\hat{H}_{\mathbf{k}} = \frac{1}{2}(\hat{\mathbf{p}} + \mathbf{k})^2 + \hat{V}_{\mathbf{k}}, \quad (3.5)$$

with

$$\hat{H}_{\mathbf{k}} |n\mathbf{k}\rangle = \epsilon_{n\mathbf{k}} |n\mathbf{k}\rangle, \quad (3.6)$$

where  $\hat{V}_{\mathbf{k}} = \hat{V}^l + \hat{V}_{\mathbf{k}}^{\text{nl}}$ ;  $\hat{V}^l$  and  $\hat{V}_{\mathbf{k}}^{\text{nl}}$  are the local and nonlocal parts of the potential, respectively. Specializing Eq. (A9) to the periodic potential of the crystal, we find the first-order correction to the Hamiltonian, which also operates on state  $|n\mathbf{k}\rangle$ , can be written as

$$\hat{H}_{\mathbf{k}\mathbf{q}}^{(1)} = \alpha[\mathbf{A}_{\mathbf{q}} \cdot \nabla_{\mathbf{k}} \hat{H}_{\mathbf{k}} + \frac{1}{2} \mathbf{A}_{\mathbf{q}} \cdot \nabla_{\mathbf{k}} (\mathbf{q} \cdot \nabla_{\mathbf{k}} \hat{H}_{\mathbf{k}})] + O(q^2). \quad (3.7)$$

The charge current operator which is coupled to  $\mathbf{A}_{\mathbf{q}}$  in the above Hamiltonian is

$$\hat{\mathcal{J}}_{\mathbf{k}\mathbf{q}}^{(0)} = -\nabla_{\mathbf{k}} \hat{H}_{\mathbf{k}} - \frac{1}{2} \nabla_{\mathbf{k}} (\mathbf{q} \cdot \nabla_{\mathbf{k}} \hat{H}_{\mathbf{k}}) + O(q^2). \quad (3.8)$$

Similarly, the induced current operator to first order in  $\mathbf{A}$  is

$$\hat{\mathcal{J}}_{\mathbf{k}\mathbf{q}}^{(1)} = -\nabla_{\mathbf{k}} \hat{H}_{\mathbf{k}\mathbf{q}}^{(1)} - \frac{1}{2} \nabla_{\mathbf{k}} (\mathbf{q} \cdot \nabla_{\mathbf{k}} \hat{H}_{\mathbf{k}\mathbf{q}}^{(1)}) + O(q^2), \quad (3.9)$$

where the minus signs in Eqs. (3.8) and (3.9) are due to the charge of the electron ( $-1$  in atomic units).

To take the Pauli principle into consideration in the single-particle formalism, we choose to derive the optical response functions with the density-matrix approach.<sup>41,42</sup> Let the particle density-matrix operator be represented by  $\hat{n}$ . (The corresponding charge density-matrix operator is denoted by  $\hat{\rho}$ .) In first-order perturbation calculation, one can write the particle density matrix as  $\hat{n} = \hat{n}^{(0)} + \hat{n}^{(1)}$ , with  $\hat{n}^{(0)}$  and  $\hat{n}^{(1)}$  being the density-matrix operators of the unperturbed and the first-order perturbed system, respectively. The Liouville equation can be written as

$$i \frac{\partial \hat{n}^{(1)}}{\partial t} = [\hat{H}, \hat{n}^{(1)}] + [\hat{H}^{(1)}, \hat{n}^{(0)}], \quad (3.10)$$

where, from the definition of the density matrix,  $\hat{n}^{(0)} |\psi_{n\mathbf{k}}\rangle = f(\epsilon_{n\mathbf{k}}) |\psi_{n\mathbf{k}}\rangle$ , with  $|\psi_{n\mathbf{k}}\rangle$  an eigenstate of the unperturbed Hamiltonian  $\hat{H}_{\mathbf{k}}$  and  $f(\epsilon_{n\mathbf{k}})$  its Fermi occupation number.

With the monochromatic assumption  $\hat{n}^{(1)} = e^{i(\mathbf{q}\cdot\mathbf{r} - \omega t)} \hat{n}_{\mathbf{q}}^{(1)}(\omega)$  and the help of Eqs. (3.5) and (3.6), Eq. (3.10) yields

$$\begin{aligned} & \langle m, \mathbf{k} + \mathbf{q} | \hat{n}_{\mathbf{q}}^{(1)}(\omega) | n\mathbf{k} \rangle \\ &= \frac{[f(\epsilon_{n\mathbf{k}}) - f(\epsilon_{m\mathbf{k}+\mathbf{q}})] \langle m, \mathbf{k} + \mathbf{q} | \hat{H}_{\mathbf{k}\mathbf{q}}^{(1)} | n\mathbf{k} \rangle}{\epsilon_{n\mathbf{k}} + \omega - \epsilon_{m\mathbf{k}+\mathbf{q}}}. \end{aligned} \quad (3.11)$$

The first-order (in  $\mathbf{A}$ ) induced electron charge density  $\rho_{\mathbf{q}}^{(1)}(\mathbf{r}, \omega)$  and current density  $\mathbf{J}_{\mathbf{q}}^{(1)}(\mathbf{r}, \omega)$  can be obtained from<sup>41</sup>

$$\rho_{\mathbf{q}}^{(1)}(\mathbf{r}, \omega) = -\text{Tr}(\hat{n}_{\mathbf{q}}^{(1)}(\omega) | \mathbf{r} \rangle \langle \mathbf{r} |) \quad (3.12)$$

and

$$\mathbf{J}_{\mathbf{q}}^{(1)}(\mathbf{r}, \omega) = \text{Tr}(\hat{n}_{\mathbf{q}}^{(1)}(\omega) \hat{\mathcal{J}}^{(0)}(\mathbf{r})) + \text{Tr}(\hat{n}^{(0)} \hat{\mathcal{J}}_{\mathbf{q}}^{(1)}(\mathbf{r}, \omega)), \quad (3.13)$$

where  $|\mathbf{r}\rangle \langle \mathbf{r}|$  is the particle-density operator in the coordinate representation and  $\hat{\mathcal{J}}^{(0)}(\mathbf{r})$  and  $\hat{\mathcal{J}}_{\mathbf{q}}^{(1)}(\mathbf{r}, \omega)$  are the charge-current-density operator for zeroth and first order in  $\mathbf{A}$ , respectively. We are interested in the long-wavelength limit without considering local-field corrections. In this limit, the induced charge and current are  $\rho_{\mathbf{q}}^{(1)}(\omega)$  and  $\mathbf{J}_{\mathbf{q}}^{(1)}(\omega)$  with

$$\rho_{\mathbf{q}}^{(1)}(\omega) = \Omega_0^{-1} \int_0 d\mathbf{r} \rho_{\mathbf{q}}^{(1)}(\mathbf{r}, \omega) \quad (3.14)$$

and

$$\mathbf{J}_{\mathbf{q}}^{(1)}(\omega) = \Omega_0^{-1} \int_0 d\mathbf{r} \mathbf{J}_{\mathbf{q}}^{(1)}(\mathbf{r}, \omega), \quad (3.15)$$

where the integration is over a unit cell and  $\Omega_0$  is the unit cell volume.

With Eqs. (3.11), (3.12), and (3.14), the induced charge density  $\rho_{\mathbf{q}}^{(1)}(\omega)$  can be written as

$$\rho_{\mathbf{q}}^{(1)}(\omega) = -\bar{\Omega}_0 \int_{\text{BZ}} d\mathbf{k} \sum_{n,m} \frac{[f(\epsilon_{n\mathbf{k}}) - f(\epsilon_{m\mathbf{k}+\mathbf{q}})] \langle n\mathbf{k} | m, \mathbf{k} + \mathbf{q} \rangle \langle m, \mathbf{k} + \mathbf{q} | \hat{H}_{\mathbf{k}\mathbf{q}}^{(1)} | n\mathbf{k} \rangle}{\epsilon_{n\mathbf{k}} + \omega - \epsilon_{m\mathbf{k}+\mathbf{q}}}, \quad (3.16)$$

where we have defined  $\bar{\Omega}_0 = \Omega_0 / (2\pi)^3$ . Likewise, with Eqs. (3.8), (3.9), and (3.11), the induced charge current density for electrons  $\mathbf{J}_{\mathbf{q}}^{(1)}(\omega)$  can be written as

$$\begin{aligned}
\mathbf{J}_q^{(1)}(\omega) &= \bar{\Omega}_0 \int_{\text{BZ}} d\mathbf{k} \left\{ \sum_{n,m} \frac{[f(\epsilon_{n\mathbf{k}}) - f(\epsilon_{m\mathbf{k}+\mathbf{q}})] \langle n\mathbf{k} | \hat{J}_{\mathbf{k}\mathbf{q}}^{(0)} | m, \mathbf{k} + \mathbf{q} \rangle \langle m, \mathbf{k} + \mathbf{q} | \hat{H}_{\mathbf{k}\mathbf{q}}^{(1)} | n\mathbf{k} \rangle}{\epsilon_{n\mathbf{k}} + \omega - \epsilon_{m, \mathbf{k} + \mathbf{q}}} + \sum_n f(\epsilon_{n\mathbf{k}}) \langle n\mathbf{k} | \hat{J}_{\mathbf{k}\mathbf{q}}^{(1)} | n\mathbf{k} \rangle \right\} \\
&= -\alpha \bar{\Omega}_0 \int_{\text{BZ}} d\mathbf{k} \left\{ \sum_{n,m} \frac{[f(\epsilon_{n\mathbf{k}}) - f(\epsilon_{m\mathbf{k}+\mathbf{q}})] \langle n\mathbf{k} | \nabla_{\mathbf{k}} \hat{H}_{\mathbf{k}} + \frac{1}{2} \nabla_{\mathbf{k}} (\mathbf{q} \cdot \nabla_{\mathbf{k}} \hat{H}_{\mathbf{k}}) | m, \mathbf{k} + \mathbf{q} \rangle}{\epsilon_{n\mathbf{k}} + \omega - \epsilon_{m, \mathbf{k} + \mathbf{q}}} \right. \\
&\quad \times \langle m, \mathbf{k} + \mathbf{q} | \mathbf{A}_{\mathbf{q}} \cdot \nabla_{\mathbf{k}} \hat{H}_{\mathbf{k}} + \frac{1}{2} \mathbf{A}_{\mathbf{q}} \cdot \nabla_{\mathbf{k}} (\mathbf{q} \cdot \nabla_{\mathbf{k}} \hat{H}_{\mathbf{k}}) | n\mathbf{k} \rangle \\
&\quad \left. + \sum_n f(\epsilon_{n\mathbf{k}}) \langle n\mathbf{k} | \nabla_{\mathbf{k}} (\mathbf{A}_{\mathbf{q}} \cdot \nabla_{\mathbf{k}} \hat{H}_{\mathbf{k}}) + \nabla_{\mathbf{k}} [\mathbf{q} \cdot \nabla_{\mathbf{k}} (\mathbf{A}_{\mathbf{q}} \cdot \nabla_{\mathbf{k}} \hat{H}_{\mathbf{k}})] | n\mathbf{k} \rangle + O(q^2) \right\}. \tag{3.17}
\end{aligned}$$

In semiconductors or insulators, the Fermi surface is specified by the band index and is independent of the Bloch wave vector  $\mathbf{k}$ . We can therefore write the Fermi occupation number  $f(\epsilon_{n\mathbf{k}})$  as  $f_n$  and  $f(\epsilon_{m\mathbf{k}+\mathbf{q}})$  as  $f_m$ . To further simplify the equation, one may (i) consider only zero temperature and (ii) replace  $\mathbf{k} + \mathbf{q}$  by  $-\mathbf{k}$  under the summation in the  $f_n = 1$  term of Eq. (3.16). The valence- and conduction-band states ( $f_n = 1$  and 0, respectively) will be referred to with the symbols  $v$  and  $c$ . For derivation of the dielectric function and the optical activity tensor, we need only expand Eqs. (3.16) and (3.17) to first order in  $q$ . We use the following relations, which hold to first order in  $q$ ,

$$\nabla_{\mathbf{k}} \hat{H}_{\mathbf{k}-\mathbf{q}} = \nabla_{\mathbf{k}} \hat{H}_{\mathbf{k}} - \nabla_{\mathbf{k}} (\mathbf{q} \cdot \nabla_{\mathbf{k}} \hat{H}_{\mathbf{k}}), \tag{3.18}$$

$$\nabla_{\mathbf{k}} (\mathbf{q} \cdot \nabla_{\mathbf{k}} \hat{H}_{\mathbf{k}-\mathbf{q}}) = \nabla_{\mathbf{k}} (\mathbf{q} \cdot \nabla_{\mathbf{k}} \hat{H}_{\mathbf{k}}) \tag{3.19}$$

and time-reversal symmetry<sup>43</sup> (specifically,  $\epsilon_{n\mathbf{k}} = \epsilon_{n, -\mathbf{k}}$  and  $\langle n, -\mathbf{k} | m, -\mathbf{k} \rangle = \langle m\mathbf{k} | n\mathbf{k} \rangle$ ) to transform Eq. (3.16) into

$$\begin{aligned}
\rho_q^{(1)}(\omega) &= \alpha \bar{\Omega}_0 \int_{\text{BZ}} d\mathbf{k} \sum_n^v \sum_m^c \sum_{\pm} \pm \frac{\langle m\mathbf{k} | n, \mathbf{k} + \mathbf{q} \rangle \langle n, \mathbf{k} + \mathbf{q} | \mathbf{A}_{\mathbf{q}} \cdot \nabla_{\mathbf{k}} \hat{H}_{\mathbf{k}} + \frac{1}{2} \mathbf{A}_{\mathbf{q}} \cdot \nabla_{\mathbf{k}} (\mathbf{q} \cdot \nabla_{\mathbf{k}} \hat{H}_{\mathbf{k}}) + O(q^2) | m\mathbf{k} \rangle}{\epsilon_{n, \mathbf{k} + \mathbf{q}} \pm \omega - \epsilon_{m\mathbf{k}}} \\
&= -2\alpha\omega \bar{\Omega}_0 \int_{\text{BZ}} d\mathbf{k} \sum_n^v \sum_m^c \frac{\langle m\mathbf{k} | n, \mathbf{k} + \mathbf{q} \rangle \langle n, \mathbf{k} + \mathbf{q} | \mathbf{A}_{\mathbf{q}} \cdot \nabla_{\mathbf{k}} \hat{H}_{\mathbf{k}} + \frac{1}{2} \mathbf{A}_{\mathbf{q}} \cdot \nabla_{\mathbf{k}} (\mathbf{q} \cdot \nabla_{\mathbf{k}} \hat{H}_{\mathbf{k}}) + O(q^2) | m\mathbf{k} \rangle}{(\epsilon_{n, \mathbf{k} + \mathbf{q}} + \omega - \epsilon_{m\mathbf{k}})(\epsilon_{n, \mathbf{k} + \mathbf{q}} - \omega - \epsilon_{m\mathbf{k}})}. \tag{3.20}
\end{aligned}$$

Following similar procedures, we can rewrite Eq. (3.17) as

$$\begin{aligned}
\mathbf{J}_q^{(1)}(\omega) &= -\alpha \bar{\Omega}_0 \int_{\text{BZ}} d\mathbf{k} \left\{ \sum_n^v \sum_m^c 2(\epsilon_{n, \mathbf{k} + \mathbf{q}} - \epsilon_{m\mathbf{k}}) \frac{\langle m\mathbf{k} | \nabla_{\mathbf{k}} \hat{H}_{\mathbf{k}} + \frac{1}{2} \nabla_{\mathbf{k}} (\mathbf{q} \cdot \nabla_{\mathbf{k}} \hat{H}_{\mathbf{k}}) | n, \mathbf{k} + \mathbf{q} \rangle}{(\epsilon_{n, \mathbf{k} + \mathbf{q}} + \omega - \epsilon_{m\mathbf{k}})(\epsilon_{n, \mathbf{k} + \mathbf{q}} - \omega - \epsilon_{m\mathbf{k}})} \right. \\
&\quad \times \langle n, \mathbf{k} + \mathbf{q} | \mathbf{A}_{\mathbf{q}} \cdot \nabla_{\mathbf{k}} \hat{H}_{\mathbf{k}} + \frac{1}{2} \mathbf{A}_{\mathbf{q}} \cdot \nabla_{\mathbf{k}} (\mathbf{q} \cdot \nabla_{\mathbf{k}} \hat{H}_{\mathbf{k}}) | m\mathbf{k} \rangle \\
&\quad \left. + \sum_n^v \langle n\mathbf{k} | \nabla_{\mathbf{k}} (\mathbf{A}_{\mathbf{q}} \cdot \nabla_{\mathbf{k}} \hat{H}_{\mathbf{k}}) + \nabla_{\mathbf{k}} [\mathbf{q} \cdot \nabla_{\mathbf{k}} (\mathbf{A}_{\mathbf{q}} \cdot \nabla_{\mathbf{k}} \hat{H}_{\mathbf{k}})] | n\mathbf{k} \rangle + O(q^2) \right\}. \tag{3.21}
\end{aligned}$$

To obtain the dielectric function and the optical activity tensor in the long-wavelength limit, we compare the microscopic expression for the current with the macroscopic relation, Eq. (2.10). We need to expand the microscopic expression Eq. (3.21) to first order in  $q$ . First-order  $\mathbf{k} \cdot \mathbf{p}$  perturbation theory gives

$$|n, \mathbf{k} + \mathbf{q}\rangle = |n\mathbf{k}\rangle + G_{n\mathbf{k}}(\mathbf{q} \cdot \nabla_{\mathbf{k}} \hat{H}_{\mathbf{k}}) | n\mathbf{k}\rangle + O(q^2) \tag{3.22}$$

and

$$\epsilon_{n, \mathbf{k} + \mathbf{q}} = \epsilon_{n\mathbf{k}} + \mathbf{q} \cdot \nabla_{\mathbf{k}} \epsilon_{n\mathbf{k}} + O(q^2), \tag{3.23}$$

where  $G_{n\mathbf{k}} = G_{n\mathbf{k}}(0)$  is the Green function at zero frequency. The frequency-dependent Green function is defined as

$$G_{n\mathbf{k}}(\omega) = \sum_{m \neq n} \frac{|m\mathbf{k}\rangle \langle m\mathbf{k}|}{\epsilon_{n\mathbf{k}} + \omega - \epsilon_{m\mathbf{k}}}. \tag{3.24}$$

In Eq. (3.24) the intermediate state  $m$  can be in either a valence or conduction band. If the intermediate states are restricted to valence bands, we use a superscript  $v$  on the Green function; if restricted to the conduction bands, the superscript is  $c$ . If not specified, for example, as in Eq. (3.22), relation  $G_{n\mathbf{k}} = G_{n\mathbf{k}}^v + G_{n\mathbf{k}}^c$  holds.

In order to indicate the orders both in  $\mathbf{A}$  and  $\mathbf{q}$ , two superscripts are used; the first superscript indicates the order of  $\mathbf{A}$  and the second the order of  $\mathbf{q}$ ; for example,  $\rho^{(n,m)}$  is the induced charge density of  $n$ th order in  $\mathbf{A}$  and  $m$ th order in  $\mathbf{q}$ . It is straightforward to show from Eq. (3.20) that to zeroth order in  $\mathbf{q}$  the induced charge density vanishes by observing that the wave functions of the conduction band  $m$  and valence band  $n$  are orthogonal:

$$\rho_q^{(1,0)}(\omega) = -2\alpha\omega\bar{\Omega}_0 \int_{\text{BZ}} d\mathbf{k} \sum_n^v \sum_m^c \frac{\langle m\mathbf{k}|n\mathbf{k}\rangle \langle n\mathbf{k}|\mathbf{A}_q \cdot \nabla_k \hat{H}_k|m\mathbf{k}\rangle}{(\epsilon_{n\mathbf{k}} + \omega - \epsilon_{m\mathbf{k}})(\epsilon_{n\mathbf{k}} - \omega - \epsilon_{m\mathbf{k}})} = 0. \quad (3.25)$$

With Eqs. (3.16), (3.22), and (3.23), we obtain the induced density to first order in  $q$ ,

$$\begin{aligned} \rho_q^{(1,1)}(\omega) &= -2\alpha\omega\bar{\Omega}_0 \int_{\text{BZ}} d\mathbf{k} \sum_n^v \sum_m^c \frac{\langle m\mathbf{k}|G_{n\mathbf{k}}(\mathbf{q} \cdot \nabla_k \hat{H}_k)|n\mathbf{k}\rangle \langle n\mathbf{k}|\mathbf{A}_q \cdot \nabla_k \hat{H}_k|m\mathbf{k}\rangle}{(\epsilon_{n\mathbf{k}} + \omega - \epsilon_{m\mathbf{k}})(\epsilon_{n\mathbf{k}} - \omega - \epsilon_{m\mathbf{k}})} \\ &= -2\alpha\omega\bar{\Omega}_0 \int_{\text{BZ}} d\mathbf{k} \sum_n^v \langle n\mathbf{k} | (\mathbf{A}_q \cdot \nabla_k \hat{H}_k) G_{n\mathbf{k}}^c(\omega) G_{n\mathbf{k}}^c(-\omega) G_{n\mathbf{k}}^c(\mathbf{q} \cdot \nabla_k \hat{H}_k) | n\mathbf{k} \rangle, \end{aligned} \quad (3.26)$$

noting that  $G_{n\mathbf{k}}^c(\omega) G_{n\mathbf{k}}^c(-\omega) = \sum_m^c |m\mathbf{k}\rangle \langle m\mathbf{k}| / (\epsilon_{n\mathbf{k}} + \omega - \epsilon_{m\mathbf{k}})(\epsilon_{n\mathbf{k}} - \omega - \epsilon_{m\mathbf{k}})$ .

To zeroth order in  $q$ , the induced current density from Eq. (3.21) is

$$\begin{aligned} \mathbf{J}_q^{(1,0)}(\omega) &= -\alpha\Omega_0 \int_{\text{BZ}} d\mathbf{k} \left\{ \sum_n^v \sum_m^c 2(\epsilon_{n\mathbf{k}} - \epsilon_{m\mathbf{k}}) \frac{\langle m\mathbf{k}|\nabla_k \hat{H}_k|n\mathbf{k}\rangle \langle n\mathbf{k}|\mathbf{A}_q \cdot \nabla_k \hat{H}_k|m\mathbf{k}\rangle}{(\epsilon_{n\mathbf{k}} + \omega - \epsilon_{m\mathbf{k}})(\epsilon_{n\mathbf{k}} - \omega - \epsilon_{m\mathbf{k}})} + \sum_n^v \langle n\mathbf{k}|\nabla_k(\mathbf{A}_q \cdot \nabla_k \hat{H}_k)|n\mathbf{k}\rangle \right\} \\ &= -\alpha\bar{\Omega}_0 \int_{\text{BZ}} d\mathbf{k} \sum_n^v \left\{ \sum_{\pm} \langle n\mathbf{k}|\mathbf{A}_q \cdot \nabla_k \hat{H}_k G_{n\mathbf{k}}^c(\pm\omega) \nabla_k \hat{H}_k | n\mathbf{k} \rangle + \langle n\mathbf{k}|\nabla_k(\mathbf{A}_q \cdot \nabla_k \hat{H}_k)|n\mathbf{k}\rangle \right\}. \end{aligned} \quad (3.27)$$

Also from Eq. (3.21), the induced-current density to first-order in  $q$  can be written as

$$\begin{aligned} \mathbf{J}_q^{(1,1)}(\omega) &= -2\alpha\bar{\Omega}_0 \int_{\text{BZ}} d\mathbf{k} \sum_n^v \left\{ \langle n\mathbf{k}|\mathbf{A}_q \cdot \nabla_k \hat{H}_k(\epsilon_{n\mathbf{k}} - \hat{H}_k) G_{n\mathbf{k}}^c(\omega) G_{n\mathbf{k}}^c(-\omega) \frac{1}{2} \nabla_k(\mathbf{q} \cdot \nabla_k \hat{H}_k) | n\mathbf{k} \rangle \right. \\ &\quad + \langle n\mathbf{k}|\frac{1}{2} \mathbf{A}_q \cdot \nabla_k(\mathbf{q} \cdot \nabla_k \hat{H}_k)(\epsilon_{n\mathbf{k}} - \hat{H}_k) G_{n\mathbf{k}}^c(\omega) G_{n\mathbf{k}}^c(-\omega) \nabla_k \hat{H}_k | n\mathbf{k} \rangle \\ &\quad + \langle n\mathbf{k}|\mathbf{A}_q \cdot \nabla_k \hat{H}_k(\epsilon_{n\mathbf{k}} - \hat{H}_k) G_{n\mathbf{k}}^c(\omega) G_{n\mathbf{k}}^c(-\omega) \nabla_k \hat{H}_k G_{n\mathbf{k}} \mathbf{q} \cdot \nabla_k \hat{H}_k | n\mathbf{k} \rangle \\ &\quad + \langle n\mathbf{k}|\mathbf{q} \cdot \nabla_k \hat{H}_k G_{n\mathbf{k}} \mathbf{A}_q \cdot \nabla_k \hat{H}_k(\epsilon_{n\mathbf{k}} - \hat{H}_k) G_{n\mathbf{k}}^c(\omega) G_{n\mathbf{k}}^c(-\omega) \nabla_k \hat{H}_k | n\mathbf{k} \rangle \\ &\quad \left. - \langle n\mathbf{k}|\mathbf{A}_q \cdot \nabla_k \hat{H}_k[(\epsilon_{n\mathbf{k}} - \hat{H}_k)^2 + \omega^2][G_{n\mathbf{k}}^c(\omega) G_{n\mathbf{k}}^c(-\omega)]^2 \nabla_k \hat{H}_k | n\mathbf{k} \rangle \langle n\mathbf{k}|\mathbf{q} \cdot \nabla_k \hat{H}_k | n\mathbf{k} \rangle \right\}. \end{aligned} \quad (3.28)$$

Equations (3.25)–(3.28) are obtained by directly expanding Eq. (3.20) or (3.21) and collecting all the terms which are zeroth or first order in  $q$ .

Equations (3.27) and (3.28) can be used to extract the expressions of the dielectric function and the optical activity tensor by comparing with Eq. (2.10). Define the linear susceptibility  $\chi_{ij}$  from the relation

$$\epsilon_{ij} \equiv \delta_{ij} + 4\pi\chi_{ij}. \quad (3.29)$$

We obtain from Eq. (3.27),

$$\chi_{ij} = -\frac{\bar{\Omega}_0}{\omega^2} \int_{\text{BZ}} d\mathbf{k} \sum_n^v \left\{ \sum_{\pm} \langle n\mathbf{k}|\hat{\mathbf{i}} \cdot \nabla_k \hat{H}_k G_{n\mathbf{k}}^c(\pm\omega) \hat{\mathbf{j}} \cdot \nabla_k \hat{H}_k | n\mathbf{k} \rangle + \langle n\mathbf{k}|\hat{\mathbf{i}} \cdot \nabla_k \hat{\mathbf{j}} \cdot (\nabla_k \hat{H}_k) | n\mathbf{k} \rangle \right\} \quad (3.30)$$

and from Eq. (3.27),

$$\begin{aligned} i\eta_{ijkl} &= -\frac{8\pi\bar{\Omega}_0}{\omega^2} \int_{\text{BZ}} d\mathbf{k} \sum_n^v \left\{ \langle n\mathbf{k}|\hat{\mathbf{l}} \cdot \nabla_k \hat{H}_k(\epsilon_{n\mathbf{k}} - \hat{H}_k) G_{n\mathbf{k}}^c(\omega) G_{n\mathbf{k}}^c(-\omega) \frac{1}{2} \hat{\mathbf{i}} \cdot \nabla_k(\hat{\mathbf{j}} \cdot \nabla_k \hat{H}_k) | n\mathbf{k} \rangle \right. \\ &\quad + \langle n\mathbf{k}|\frac{1}{2} \hat{\mathbf{l}} \cdot \nabla_k(\hat{\mathbf{j}} \cdot \nabla_k \hat{H}_k)(\epsilon_{n\mathbf{k}} - \hat{H}_k) G_{n\mathbf{k}}^c(\omega) G_{n\mathbf{k}}^c(-\omega) \hat{\mathbf{i}} \cdot \nabla_k \hat{H}_k | n\mathbf{k} \rangle \\ &\quad + \langle n\mathbf{k}|\hat{\mathbf{l}} \cdot \nabla_k \hat{H}_k(\epsilon_{n\mathbf{k}} - \hat{H}_k) G_{n\mathbf{k}}^c(\omega) G_{n\mathbf{k}}^c(-\omega) \hat{\mathbf{i}} \cdot \nabla_k \hat{H}_k G_{n\mathbf{k}} \hat{\mathbf{j}} \cdot \nabla_k \hat{H}_k | n\mathbf{k} \rangle \\ &\quad + \langle n\mathbf{k}|\hat{\mathbf{j}} \cdot \nabla_k \hat{H}_k G_{n\mathbf{k}} \hat{\mathbf{l}} \cdot \nabla_k \hat{H}_k(\epsilon_{n\mathbf{k}} - \hat{H}_k) G_{n\mathbf{k}}^c(\omega) G_{n\mathbf{k}}^c(-\omega) \hat{\mathbf{i}} \cdot \nabla_k \hat{H}_k | n\mathbf{k} \rangle \\ &\quad \left. - \langle n\mathbf{k}|\hat{\mathbf{l}} \cdot \nabla_k \hat{H}_k[(\epsilon_{n\mathbf{k}} - \hat{H}_k)^2 + \omega^2][G_{n\mathbf{k}}^c(\omega) G_{n\mathbf{k}}^c(-\omega)]^2 \hat{\mathbf{i}} \cdot \nabla_k \hat{H}_k | n\mathbf{k} \rangle \langle n\mathbf{k}|\hat{\mathbf{j}} \cdot \nabla_k \hat{H}_k | n\mathbf{k} \rangle \right\}. \end{aligned} \quad (3.31)$$

The optical activity tensor  $\eta$  has units of length; in the equation above, it takes the atomic unit of length, bohr.

### C. Symmetries and sum rules

An important check on the microscopic formulas is to see if the quantities derived have the desired symmetry properties obtained from the macroscopic theory. The dielectric function  $\epsilon_{ij}$  and the susceptibility  $\chi_{ij}$  are real symmetric matrices, while  $\eta_{ijk}$  is real and antisymmetric in the first and third indices.<sup>25</sup> We can use time-reversal symmetry to show that  $\chi$  and  $\eta$  of Eqs. (3.30) and (3.31) have the desired symmetry properties.

If the Hamiltonian is invariant under time-reversal symmetry, it has been shown<sup>43</sup> that  $\epsilon_{nk} = \epsilon_{n,-k}$  and  $\langle \mathbf{r} | n, \mathbf{k} \rangle = \langle \mathbf{r} | n, -\mathbf{k} \rangle^*$ . With Eq. (3.5), it is easy to show

that the relation

$$\langle n, -\mathbf{k} | \nabla_{-\mathbf{k}} \hat{H}_{-\mathbf{k}} | m, -\mathbf{k} \rangle = -\langle n\mathbf{k} | \nabla_{\mathbf{k}} \hat{H}_{\mathbf{k}} | m\mathbf{k} \rangle^* \quad (3.32)$$

holds. In Eqs. (3.30) and (3.31), one can freely change the dummy integration variable  $\mathbf{k}$  to  $-\mathbf{k}$  for all the terms in the Brillouin-zone integration. Writing out the Green function as shown in Eq. (3.24) and using Eq. (3.32), one can obtain  $\chi_{ij} = \chi_{ij}^*$  and  $\eta_{ijl} = \eta_{ijl}^*$ , or  $\chi_{ij} = \chi_{ji}$  and  $\eta_{ijl} = -\eta_{lji}$ , which are the desired symmetry properties from the macroscopic theory.

For any complex quantity  $x$ ,  $\text{Re}(x) = \frac{1}{2}(x + x^*)$  and  $\text{Im}(x) = (1/2i)(x - x^*)$ . With the use of these identities and Eq. (3.32), the linear susceptibility, Eq. (3.30), can be rewritten as

$$\chi_{ij} = -\frac{\bar{\Omega}_0}{\omega^2} \int_{\text{BZ}} d\mathbf{k} \sum_n^v \text{Re} \left\{ \sum_{\pm} \langle n\mathbf{k} | \hat{\mathbf{i}} \cdot \nabla_{\mathbf{k}} \hat{H}_{\mathbf{k}} G_{n\mathbf{k}}^c(\pm\omega) \hat{\mathbf{j}} \cdot (\nabla_{\mathbf{k}} \hat{H}_{\mathbf{k}}) | n\mathbf{k} \rangle + \langle n\mathbf{k} | \hat{\mathbf{i}} \cdot \nabla_{\mathbf{k}} \hat{\mathbf{j}} \cdot \nabla_{\mathbf{k}} \hat{H}_{\mathbf{k}} | n\mathbf{k} \rangle \right\}, \quad (3.33)$$

and the optical activity tensor, Eq. (3.31), becomes

$$\begin{aligned} \eta_{ijl} = & -\frac{8\pi\bar{\Omega}_0}{\omega^2} \int_{\text{BZ}} d\mathbf{k} \sum_n^v \text{Im} \{ \langle n\mathbf{k} | \hat{\mathbf{l}} \cdot \nabla_{\mathbf{k}} \hat{H}_{\mathbf{k}} (\epsilon_{n\mathbf{k}} - \hat{H}_{\mathbf{k}}) G_{n\mathbf{k}}^c(\omega) G_{n\mathbf{k}}^c(-\omega) \frac{1}{2} \hat{\mathbf{i}} \cdot \nabla_{\mathbf{k}} (\hat{\mathbf{j}} \cdot \nabla_{\mathbf{k}} \hat{H}_{\mathbf{k}}) | n\mathbf{k} \rangle \\ & + \langle n\mathbf{k} | \frac{1}{2} \hat{\mathbf{l}} \cdot \nabla_{\mathbf{k}} (\hat{\mathbf{j}} \cdot \nabla_{\mathbf{k}} \hat{H}_{\mathbf{k}}) (\epsilon_{n\mathbf{k}} - \hat{H}_{\mathbf{k}}) G_{n\mathbf{k}}^c(\omega) G_{n\mathbf{k}}^c(-\omega) \hat{\mathbf{i}} \cdot \nabla_{\mathbf{k}} \hat{H}_{\mathbf{k}} | n\mathbf{k} \rangle \\ & + \langle n\mathbf{k} | \hat{\mathbf{l}} \cdot \nabla_{\mathbf{k}} \hat{H}_{\mathbf{k}} (\epsilon_{n\mathbf{k}} - \hat{H}_{\mathbf{k}}) G_{n\mathbf{k}}^c(\omega) G_{n\mathbf{k}}^c(-\omega) \hat{\mathbf{i}} \cdot \nabla_{\mathbf{k}} \hat{H}_{\mathbf{k}} G_{n\mathbf{k}} \hat{\mathbf{j}} \cdot \nabla_{\mathbf{k}} \hat{H}_{\mathbf{k}} | n\mathbf{k} \rangle \\ & + \langle n\mathbf{k} | \hat{\mathbf{j}} \cdot \nabla_{\mathbf{k}} \hat{H}_{\mathbf{k}} G_{n\mathbf{k}} \hat{\mathbf{l}} \cdot \nabla_{\mathbf{k}} \hat{H}_{\mathbf{k}} (\epsilon_{n\mathbf{k}} - \hat{H}_{\mathbf{k}}) G_{n\mathbf{k}}^c(\omega) G_{n\mathbf{k}}^c(-\omega) \hat{\mathbf{i}} \cdot \nabla_{\mathbf{k}} \hat{H}_{\mathbf{k}} | n\mathbf{k} \rangle \\ & - \langle n\mathbf{k} | \hat{\mathbf{l}} \cdot \nabla_{\mathbf{k}} \hat{H}_{\mathbf{k}} [(\epsilon_{n\mathbf{k}} - \hat{H}_{\mathbf{k}})^2 + \omega^2] [G_{n\mathbf{k}}^c(\omega) G_{n\mathbf{k}}^c(-\omega)] \hat{\mathbf{i}} \cdot \nabla_{\mathbf{k}} \hat{H}_{\mathbf{k}} | n\mathbf{k} \rangle \langle n\mathbf{k} | \hat{\mathbf{j}} \cdot \nabla_{\mathbf{k}} \hat{H}_{\mathbf{k}} | n\mathbf{k} \rangle \}. \end{aligned} \quad (3.34)$$

Next we show sum rules for the dielectric constants and the optical-activity tensor. With the use of these sum rules, the dielectric constant and the optical activity tensor have well-defined  $\omega \rightarrow 0$  limits. Consider a system under the influence of a static field described by

$$\mathbf{A} = \mathbf{A}_q e^{iq \cdot \mathbf{r}}. \quad (3.35)$$

The Maxwell equations show that there is no electric field under the assumption Eq. (3.35) in the  $\phi=0$  gauge. The induced current  $\mathbf{J}$  is given by  $\mathbf{J} = (1/4\pi\alpha)(\nabla \times \mathbf{B}) = (1/4\pi\alpha)[\nabla \times (\nabla \times \mathbf{A})]$ . Using Eq. (3.35), we obtain

$$\mathbf{J}_q = \frac{1}{4\pi\alpha} [q^2 \mathbf{A}_q - \mathbf{q}(\mathbf{q} \cdot \mathbf{A}_q)]. \quad (3.36)$$

The above equation shows that in powers of  $q$ , the first nonvanishing induced current due to the influence of a static field is of order  $q^2$ . In other words, the induced current to the zeroth and first order of  $q$  must vanish. Using Eq. (3.27), for the current to zeroth order in  $q$ , we obtain a sum rule

$$\int_{\text{BZ}} d\mathbf{k} \sum_n^v \{ \langle n\mathbf{k} | \hat{\mathbf{i}} \cdot \nabla_{\mathbf{k}} \hat{H}_{\mathbf{k}} G_{n\mathbf{k}}^c \hat{\mathbf{j}} \cdot \nabla_{\mathbf{k}} \hat{H}_{\mathbf{k}} | n\mathbf{k} \rangle + \frac{1}{2} \langle n\mathbf{k} | \hat{\mathbf{i}} \cdot \nabla_{\mathbf{k}} \hat{\mathbf{j}} \cdot (\nabla_{\mathbf{k}} \hat{H}_{\mathbf{k}}) | n\mathbf{k} \rangle \} = 0, \quad (3.37)$$

where the induced current is taken to be in the  $\hat{\mathbf{i}}$  direction and  $\mathbf{A}_q$  in the  $\hat{\mathbf{j}}$  direction in Eq. (3.27). This is equivalent to Eq. (2.33) of Ref. 20. Similarly, Eq. (3.28) for the current, to first order in  $q$ , leads to the sum rule

$$\begin{aligned} \int_{\text{BZ}} d\mathbf{k} \sum_n^v \{ \langle n\mathbf{k} | \hat{\mathbf{l}} \cdot \nabla_{\mathbf{k}} \hat{H}_{\mathbf{k}} G_{n\mathbf{k}}^c \frac{1}{2} \hat{\mathbf{i}} \cdot \nabla_{\mathbf{k}} (\hat{\mathbf{j}} \cdot \nabla_{\mathbf{k}} \hat{H}_{\mathbf{k}}) | n\mathbf{k} \rangle + \langle n\mathbf{k} | \frac{1}{2} \hat{\mathbf{l}} \cdot \nabla_{\mathbf{k}} (\hat{\mathbf{j}} \cdot \nabla_{\mathbf{k}} \hat{H}_{\mathbf{k}}) G_{n\mathbf{k}}^c \hat{\mathbf{i}} \cdot \nabla_{\mathbf{k}} \hat{H}_{\mathbf{k}} | n\mathbf{k} \rangle \\ + \langle n\mathbf{k} | \hat{\mathbf{l}} \cdot \nabla_{\mathbf{k}} \hat{H}_{\mathbf{k}} G_{n\mathbf{k}}^c \hat{\mathbf{i}} \cdot \nabla_{\mathbf{k}} \hat{H}_{\mathbf{k}} G_{n\mathbf{k}} \hat{\mathbf{j}} \cdot \nabla_{\mathbf{k}} \hat{H}_{\mathbf{k}} | n\mathbf{k} \rangle + \langle n\mathbf{k} | \hat{\mathbf{j}} \cdot \nabla_{\mathbf{k}} \hat{H}_{\mathbf{k}} G_{n\mathbf{k}} \hat{\mathbf{l}} \cdot \nabla_{\mathbf{k}} \hat{H}_{\mathbf{k}} G_{n\mathbf{k}}^c \hat{\mathbf{i}} \cdot \nabla_{\mathbf{k}} \hat{H}_{\mathbf{k}} | n\mathbf{k} \rangle \\ - \langle n\mathbf{k} | \hat{\mathbf{l}} \cdot \nabla_{\mathbf{k}} \hat{H}_{\mathbf{k}} (G_{n\mathbf{k}}^c)^2 \hat{\mathbf{i}} \cdot \nabla_{\mathbf{k}} \hat{H}_{\mathbf{k}} | n\mathbf{k} \rangle \langle n\mathbf{k} | \hat{\mathbf{j}} \cdot \nabla_{\mathbf{k}} \hat{H}_{\mathbf{k}} | n\mathbf{k} \rangle \} = 0, \end{aligned} \quad (3.38)$$

where  $\mathbf{J}_q^{(1,1)}$  is taken to be in the  $\hat{\mathbf{i}}$  direction,  $\mathbf{q}$  in the  $\hat{\mathbf{j}}$  direction, and  $\mathbf{A}_q$  in the  $\hat{\mathbf{l}}$  direction. With the help of the sum

rules Eqs. (3.37) and (3.38), we can explicitly show that formulas for  $\chi$  and  $\eta$ , which are applicable only to semiconductors, have no apparent divergence in the static limit. Subtracting Eq. (3.37) from Eq. (3.33), Eq. (3.38) from Eq. (3.31), and using the relation

$$(\epsilon_{nk} - \hat{H}_k)G_{nk}(\omega)G_{nk}(-\omega) - G_{nk} = \omega^2 G_{nk}(\omega)G_{nk}(-\omega)G_{nk} = \omega^2 \mathcal{G}_{nk}(\omega), \quad (3.39)$$

where we have defined

$$\mathcal{G}_{nk}(\omega) \equiv G_{nk}(\omega)G_{nk}(-\omega)G_{nk} \quad (3.40)$$

and

$$[(\epsilon_{nk} - \hat{H}_k)^2 + \omega^2]G_{nk}^2(\omega)G_{nk}^2(-\omega) - G_{nk}^2 = \omega^2[3(\epsilon_{nk} - \hat{H}_k)^2 - \omega^2]\mathcal{G}_{nk}^2(\omega), \quad (3.41)$$

we obtain

$$\chi_{ij} = -2\bar{\Omega}_0 \int_{\text{BZ}} d\mathbf{k} \sum_n^v \text{Re} \langle n\mathbf{k} | \hat{\mathbf{i}} \cdot \nabla_{\mathbf{k}} \hat{H}_k \mathcal{G}_{nk}^c(\omega) \hat{\mathbf{j}} \cdot \nabla_{\mathbf{k}} \hat{H}_k | n\mathbf{k} \rangle \quad (3.42)$$

and

$$\begin{aligned} \eta_{ijl} = & -8\pi\bar{\Omega}_0 \int_{\text{BZ}} d\mathbf{k} \sum_n^v \text{Im} \{ \langle n\mathbf{k} | \hat{\mathbf{l}} \cdot \nabla_{\mathbf{k}} \hat{H}_k \mathcal{G}_{nk}^c(\omega) \frac{1}{2} \hat{\mathbf{i}} \cdot \nabla_{\mathbf{k}} (\hat{\mathbf{j}} \cdot \nabla_{\mathbf{k}} \hat{H}_k) | n\mathbf{k} \rangle \\ & + \langle n\mathbf{k} | \frac{1}{2} \hat{\mathbf{l}} \cdot \nabla_{\mathbf{k}} (\hat{\mathbf{j}} \cdot \nabla_{\mathbf{k}} \hat{H}_k) \mathcal{G}_{nk}^c(\omega) \hat{\mathbf{i}} \cdot \nabla_{\mathbf{k}} \hat{H}_k | n\mathbf{k} \rangle + \langle n\mathbf{k} | \hat{\mathbf{l}} \cdot \nabla_{\mathbf{k}} \hat{H}_k \mathcal{G}_{nk}^c(\omega) \hat{\mathbf{i}} \cdot \nabla_{\mathbf{k}} \hat{H}_k G_{nk} (\hat{\mathbf{j}} \cdot \nabla_{\mathbf{k}} \hat{H}_k) | n\mathbf{k} \rangle \\ & + \langle n\mathbf{k} | (\hat{\mathbf{j}} \cdot \nabla_{\mathbf{k}} \hat{H}_k) G_{nk} \hat{\mathbf{l}} \cdot \nabla_{\mathbf{k}} \hat{H}_k \mathcal{G}_{nk}^c(\omega) \hat{\mathbf{i}} \cdot \nabla_{\mathbf{k}} \hat{H}_k | n\mathbf{k} \rangle \\ & + \langle n\mathbf{k} | \hat{\mathbf{l}} \cdot \nabla_{\mathbf{k}} \hat{H}_k [-3(\epsilon_{nk} - \hat{H}_k)^2 + \omega^2] [\mathcal{G}_{nk}^c(\omega)]^2 \hat{\mathbf{i}} \cdot \nabla_{\mathbf{k}} \hat{H}_k | n\mathbf{k} \rangle \langle n\mathbf{k} | \hat{\mathbf{j}} \cdot \nabla_{\mathbf{k}} \hat{H}_k | n\mathbf{k} \rangle \} . \end{aligned} \quad (3.43)$$

Equation (3.42) agrees with Eq. (A17) of Ref. 20 derived with the scalar-field perturbation theory.

From the microscopic expressions for induced charge and current and the sum rules Eqs. (3.37) and (3.38), we can show that the continuity relation  $\nabla \cdot \mathbf{J} + \partial\rho/\partial t = 0$  holds to second order in  $q$ . For example, using the sum rule Eq. (3.37), we can rewrite Eq. (3.27) as

$$\mathbf{J}_q^{(1,0)}(\omega) = -2\alpha\omega^2\bar{\Omega}_0 \int_{\text{BZ}} d\mathbf{k} \sum_n^v \langle n\mathbf{k} | \mathbf{A}_q \cdot \nabla_{\mathbf{k}} \hat{H}_k G_{nk}^c(\omega) G_{nk}^c(-\omega) G_{nk}^c \nabla_{\mathbf{k}} \hat{H}_k | n\mathbf{k} \rangle . \quad (3.44)$$

By comparing Eqs. (3.26) and (3.44) one may see that the continuity relation holds to first order in  $q$ .

If the sum rule for the optical activity, Eq. (3.38), or the optical activity tensor, Eq. (3.43), is used directly in numerical evaluations, it is possible to encounter the following situation: two occupied states with almost equal energy from the Green function  $G_{nk}^v = \sum_{m \neq n}^v |m\mathbf{k}\rangle \langle m\mathbf{k}| / (\epsilon_{nk} - \epsilon_{m\mathbf{k}})$  in the third and fourth terms of Eq. (3.38) or (3.43) such that each of the two individual terms form these two states contributes a large magnitude, yet they nearly cancel when summed up. This type of the situation greatly affects the accuracy of the numerical calculation. To solve this problem, we follow Aspnes's convention<sup>44</sup> to further analyze the formulas in terms of conduction and valence contributions. In other words, with  $G_{nk} = G_{nk}^v + G_{nk}^c$ , one can divide Eq. (3.38) or (3.43) into  $ccv$ ,  $vvc$ , and  $cv$  terms, where  $ccv$  denotes that there are two  $G^c$  or two unoccupied virtual states in a term;  $vvc$  denotes there is one  $G^v$  and one  $G^c$  in a term; and  $cv$  denotes there is only one Green function,  $G^c$  in a term. A similar procedure was followed to avoid numerical difficulties for second-harmonic susceptibilities.<sup>21,22</sup>

The sum rule (3.38) can be written as

$$\sum_{ijl} = \sum_{ijl}^{vvc} + \sum_{ijl}^{ccv} + \sum_{ijl}^{cv} = 0, \quad (3.45)$$

where

$$\begin{aligned} \sum_{ijl}^{vvc} = & \int_{\text{BZ}} d\mathbf{k} \sum_n^v \{ \langle n\mathbf{k} | \hat{\mathbf{l}} \cdot \nabla_{\mathbf{k}} \hat{H}_k G_{nk}^c \hat{\mathbf{i}} \cdot \nabla_{\mathbf{k}} \hat{H}_k G_{nk}^v \hat{\mathbf{j}} \cdot \nabla_{\mathbf{k}} \hat{H}_k | n\mathbf{k} \rangle + \langle n\mathbf{k} | \hat{\mathbf{j}} \cdot \nabla_{\mathbf{k}} \hat{H}_k G_{nk}^v \hat{\mathbf{l}} \cdot \nabla_{\mathbf{k}} \hat{H}_k G_{nk}^c \hat{\mathbf{i}} \cdot \nabla_{\mathbf{k}} \hat{H}_k | n\mathbf{k} \rangle \\ & - \langle n\mathbf{k} | \hat{\mathbf{l}} \cdot \nabla_{\mathbf{k}} \hat{H}_k (G_{nk}^c)^2 \hat{\mathbf{i}} \cdot \nabla_{\mathbf{k}} \hat{H}_k | n\mathbf{k} \rangle \langle n\mathbf{k} | \hat{\mathbf{j}} \cdot \nabla_{\mathbf{k}} \hat{H}_k | n\mathbf{k} \rangle \} . \end{aligned} \quad (3.46)$$

We have included the last term (diagonal term) here, although it belongs to the  $cv$  term. These three terms can be combined together in a manner similar to Eq. (12) of Ref. 22 to obtain the  $vvc$  term,

$$\sum_{ijl}^{vvc} = - \int_{\text{BZ}} d\mathbf{k} \sum_{n,m}^v \langle n\mathbf{k} | \hat{\mathbf{l}} \cdot \nabla_{\mathbf{k}} \hat{H}_k G_{nk}^c G_{m\mathbf{k}}^c \hat{\mathbf{i}} \cdot \nabla_{\mathbf{k}} \hat{H}_k | m\mathbf{k} \rangle \langle m\mathbf{k} | \hat{\mathbf{j}} \cdot \nabla_{\mathbf{k}} \hat{H}_k | n\mathbf{k} \rangle . \quad (3.47)$$

The  $ccv$  and  $cv$  terms are straightforward and can easily be obtained from Eq. (3.38):

$$\Sigma_{ijl}^{ccv} = \int_{\text{BZ}} d\mathbf{k} \sum_n^v \{ \langle n\mathbf{k} | \hat{\mathbf{l}} \cdot \nabla_{\mathbf{k}} \hat{H}_{\mathbf{k}} G_{n\mathbf{k}}^c \hat{\mathbf{i}} \cdot \nabla_{\mathbf{k}} \hat{H}_{\mathbf{k}} G_{n\mathbf{k}}^c \hat{\mathbf{j}} \cdot \nabla_{\mathbf{k}} \hat{H}_{\mathbf{k}} | n\mathbf{k} \rangle + \langle n\mathbf{k} | \hat{\mathbf{j}} \cdot \nabla_{\mathbf{k}} \hat{H}_{\mathbf{k}} G_{n\mathbf{k}}^c \hat{\mathbf{l}} \cdot \nabla_{\mathbf{k}} \hat{H}_{\mathbf{k}} G_{n\mathbf{k}}^c \hat{\mathbf{i}} \cdot \nabla_{\mathbf{k}} \hat{H}_{\mathbf{k}} | n\mathbf{k} \rangle \} \quad (3.48)$$

and

$$\Sigma_{ijl}^{cv} = \int_{\text{BZ}} d\mathbf{k} \sum_n^v \{ \langle n\mathbf{k} | \hat{\mathbf{l}} \cdot \nabla_{\mathbf{k}} \hat{H}_{\mathbf{k}} G_{n\mathbf{k}}^c \frac{1}{2} \hat{\mathbf{i}} \cdot \nabla_{\mathbf{k}} (\hat{\mathbf{j}} \cdot \nabla_{\mathbf{k}} \hat{H}_{\mathbf{k}}) | n\mathbf{k} \rangle + \langle n\mathbf{k} | \frac{1}{2} \hat{\mathbf{l}} \cdot \nabla_{\mathbf{k}} (\hat{\mathbf{j}} \cdot \nabla_{\mathbf{k}} \hat{H}_{\mathbf{k}}) G_{n\mathbf{k}}^c \hat{\mathbf{i}} \cdot \nabla_{\mathbf{k}} \hat{H}_{\mathbf{k}} | n\mathbf{k} \rangle \} . \quad (3.49)$$

Numerically, we evaluate the quantity

$$S_{ijl} = \frac{\Sigma_{ijl}^{vvc} + \Sigma_{ijl}^{ccv} + \Sigma_{ijl}^{cv}}{|\Sigma_{ijl}^{vvc}| + |\Sigma_{ijl}^{ccv}| + |\Sigma_{ijl}^{cv}|} \quad (3.50)$$

to test the sum rule. Ideally,  $S_{ijl} = 0$ .

One can go through similar algebra and obtain from Eq. (3.43)

$$\eta_{ijl}(\omega) = \eta_{ijl}^{vvc}(\omega) + \eta_{ijl}^{ccv}(\omega) + \eta_{ijl}^{cv}(\omega) \quad (3.51)$$

with

$$\begin{aligned} \eta_{ijl}^{vvc}(\omega) = & 8\pi\bar{\Omega}_0 \int_{\text{BZ}} d\mathbf{k} \sum_{n,m}^v \text{Im} \langle n\mathbf{k} | \hat{\mathbf{j}} \cdot \nabla_{\mathbf{k}} \hat{H}_{\mathbf{k}} | m\mathbf{k} \rangle \\ & \times \langle m\mathbf{k} | \hat{\mathbf{i}} \cdot \nabla_{\mathbf{k}} \hat{H}_{\mathbf{k}} \mathcal{G}_{m\mathbf{k}}^c(\omega) [\omega^2 - (\epsilon_{m\mathbf{k}} - \hat{H}_{\mathbf{k}})^2 - (\epsilon_{n\mathbf{k}} - \hat{H}_{\mathbf{k}})^2 \\ & - (\epsilon_{m\mathbf{k}} - \hat{H}_{\mathbf{k}})(\epsilon_{n\mathbf{k}} - \hat{H}_{\mathbf{k}})] \mathcal{G}_{n\mathbf{k}}^c(\omega) \hat{\mathbf{l}} \cdot \nabla_{\mathbf{k}} \hat{H}_{\mathbf{k}} | n\mathbf{k} \rangle , \end{aligned} \quad (3.52)$$

$$\begin{aligned} \eta_{ijl}^{ccv}(\omega) = & 8\pi\bar{\Omega}_0 \int_{\text{BZ}} d\mathbf{k} \sum_n^v \text{Im} \{ \langle n\mathbf{k} | \hat{\mathbf{i}} \cdot \nabla_{\mathbf{k}} \hat{H}_{\mathbf{k}} \mathcal{G}_{n\mathbf{k}}^c(\omega) \hat{\mathbf{l}} \cdot \nabla_{\mathbf{k}} \hat{H}_{\mathbf{k}} G_{n\mathbf{k}}^c \hat{\mathbf{j}} \cdot \nabla_{\mathbf{k}} \hat{H}_{\mathbf{k}} | n\mathbf{k} \rangle \\ & - \langle n\mathbf{k} | \hat{\mathbf{l}} \cdot \nabla_{\mathbf{k}} \hat{H}_{\mathbf{k}} \mathcal{G}_{n\mathbf{k}}^c(\omega) \hat{\mathbf{i}} \cdot \nabla_{\mathbf{k}} \hat{H}_{\mathbf{k}} G_{n\mathbf{k}}^c \hat{\mathbf{j}} \cdot \nabla_{\mathbf{k}} \hat{H}_{\mathbf{k}} | n\mathbf{k} \rangle \} , \end{aligned} \quad (3.53)$$

and

$$\eta_{ijl}^{cv}(\omega) = 4\pi\bar{\Omega}_0 \int_{\text{BZ}} d\mathbf{k} \sum_n^v \text{Im} \{ \langle n\mathbf{k} | \hat{\mathbf{i}} \cdot \nabla_{\mathbf{k}} \hat{H}_{\mathbf{k}} \mathcal{G}_{n\mathbf{k}}^c(\omega) \hat{\mathbf{l}} \cdot \nabla_{\mathbf{k}} (\hat{\mathbf{j}} \cdot \nabla_{\mathbf{k}} \hat{H}_{\mathbf{k}}) | n\mathbf{k} \rangle - \langle n\mathbf{k} | \hat{\mathbf{l}} \cdot \nabla_{\mathbf{k}} \hat{H}_{\mathbf{k}} \mathcal{G}_{n\mathbf{k}}^c(\omega) \hat{\mathbf{i}} \cdot \nabla_{\mathbf{k}} (\hat{\mathbf{j}} \cdot \nabla_{\mathbf{k}} \hat{H}_{\mathbf{k}}) | n\mathbf{k} \rangle \} . \quad (3.54)$$

As shown above, we have eliminated terms such as  $1/(\epsilon_{n\mathbf{k}} - \epsilon_{m\mathbf{k}})$ , where both  $n$  and  $m$  are occupied bands from Eqs. (3.38) and (3.43). The final expression of the sum rule, Eqs. (3.47)–(3.49) and the optical activity tensor, Eqs. (3.52)–(3.54), are computationally tractable.

Finally, to obtain the formula for the optical activity tensor with the self-energy correction in the form of a scissors operator, one needs to follow the procedures similar to those shown in Refs. 20 and 22. The final expression of the optical activity tensor  $\eta_{ijl}$  can be found in Appendix B.

#### IV. OPTICAL RESPONSE FUNCTIONS OF TRIGONAL SELENIUM AND $\alpha$ -QUARTZ

##### A. Dielectric function and the second-harmonic susceptibility

Based on the LDA band-theoretical calculations and the one-electron scalar-potential perturbation theory with the self-energy effect considered at the level of the scissors operator, we have computed the dielectric constants and the nonlinear susceptibility for second-harmonic generation of trigonal selenium<sup>1</sup> and  $\alpha$ -quartz. This is a continuation of the optical response calculations of a series of semiconductors, including Si, Ge,<sup>20</sup> AIP, AlAs, GaP, and GaAs.<sup>21,22</sup> The plane-wave coefficients for the ground-state wave functions are computed by an efficient

iterative algorithm<sup>45</sup> using separable nonlocal pseudopotentials<sup>46</sup> and a rational polynomial parametrization for the local exchange-correlation functional.<sup>47</sup> The selenium pseudopotential is generated using Hamann's method,<sup>40</sup> while the oxygen and silicon pseudopotentials use two projection operators for each angular momentum<sup>48</sup> and match logarithmic derivatives over a larger energy range to enhance transferability.<sup>49</sup>

Both trigonal selenium and  $\alpha$ -quartz belong to the point group 32. Each crystal may occur in two enantiomorphs of opposite handedness, with space groups  $P3_221$  and  $P3_121$ . The calculations in this paper were conducted using the space group  $P3_221$  (with right-handed coordinates). Although there is ambiguity in the older literature, modern consensus indicates that trigonal selenium<sup>50</sup> and quartz<sup>5,12</sup> crystals in this space group produce "right-handed" or dextrorotatory rotation of the plane of polarization, i.e.,  $\rho > 0$ . Our theoretical results unambiguously produce  $\rho > 0$  for this space group for both selenium and  $\alpha$ -quartz. Right-handed optical rotation simply means that linearly polarized light has its plane of polarization rotated clockwise for light coming towards the observer. Crystals of the opposite handedness will have the opposite sign for  $\rho$ . These crystals consist of helical chains centered on a hexagonal lattice and have a threefold nonsymmorphic symmetry along the helix in the  $z$  direction and a twofold symmorphic sym-

metry along an axis which passes through a lattice site in the  $xy$  plane. Crystals belonging to this symmetry group are uniaxial with  $z$  being the optic axis. There are two independent components in both the second-harmonic tensor ( $d_{11}$  and  $d_{14}$ ) and the optical activity gyration tensor ( $g_{11}$  and  $g_{33}$ ). The relationship between the apparent handedness of the structure and the handedness of its optical rotation is not trivial, all the more so because in  $\alpha$ -quartz one can find helices of both handedness within the same crystal structure. A connection between the most polarizable helices and the handedness of optical rotation has been worked out.<sup>5</sup>

Table I shows the calculated electronic part of the dielectric constant in the static limit ( $\epsilon_\infty$ ), compared with experiment. For  $\alpha$ -quartz the small (2%) difference between the calculation of Gonze, Allan, and Teter<sup>51</sup> and ours is mostly due to the difference of the lattice constants. We use the experimental lattice constants  $a = 9.290$  bohrs and  $c = 10.215$  bohrs, and the internal atomic coordinates  $u = 0.4697$ ,  $x = 0.4135$ ,  $y = 0.2669$ , and  $z = 0.1191$  as our input parameters.<sup>52</sup>

As shown in Table I, for both selenium and  $\alpha$ -quartz, LDA overestimates the dielectric constants even when compared with the largest available experimental value. For selenium, the estimated LDA direct gap is 1.2 eV compared to the experimental band gap of the range of 2.0–2.3 eV.<sup>53</sup> There is no  $GW$  calculation available for selenium; we therefore choose the parameter in the scissors operator  $\Delta$  to be 1.1 eV. For  $\alpha$ -quartz, our LDA calculation predicts a direct gap of 6.03 eV. There is a rather wide range (from 5.6 to 11.5 eV) of experimental band gaps reported over the years.<sup>18</sup> We follow Xu and Ching<sup>18</sup> and Gonze, Allan, and Teter<sup>51</sup> in choosing  $\Delta = 1.8$  eV, which aligns the calculated optical conductivity with experiment. With the correction of the scissors operator, our calculated dielectric constants are in

agreement with experiment within the error bars.

To obtain a converged value for the dielectric constant for selenium we use a plane-wave energy cutoff of 10 hartree and a total of 144 special  $\mathbf{k}$  points in  $\frac{1}{4}$  of the Brillouin zone for the Brillouin-zone integrations. (We did not invoke the threefold nonsymmorphic symmetry in this case.) For  $\alpha$ -quartz, we need a larger energy cutoff of 23 hartree so that oxygen, which is a first-row element, is adequately described. As  $\alpha$ -quartz, an insulator, has a much wider band gap than the semiconductor selenium, we need fewer  $\mathbf{k}$  points to sample the Brillouin zone. We found 18  $\mathbf{k}$  points in  $\frac{1}{4}$  of the Brillouin zone<sup>54</sup> to be sufficient for a converged calculation.

We also calculated the frequency-dependent dielectric functions for frequencies well below the absorption edge. Figures 1–4 show the frequency-dependent ordinary and extraordinary dielectric function of trigonal selenium and  $\alpha$ -quartz. The single-oscillator model<sup>10</sup> suggests that  $[\epsilon_o(\omega) - 1]^{-1}$  or  $[\epsilon_e(\omega) - 1]^{-1}$  is a linear function of the frequency squared  $\omega^2$ . As shown in the figures, LDA calculations with or without the scissors operator comply with the single-oscillator model quite well. The experimental data for the ordinary and extraordinary dielectric function of selenium shown in Figs. 1 and 2 in the low-frequency range<sup>55</sup> suggest a straight line. There are only two data points in the high-frequency range.<sup>53</sup> These two sets of experimental data unfortunately do not line up with each other. For  $\alpha$ -quartz, as shown in Figs. 3 and 4, there are also two sets of experimental data;<sup>56,57</sup> data in the higher-frequency range do suggest a straight line. At the lowest frequencies, the curvature away from the straight line is readily explained by the onset of phonons participating in the screening of the electric field. This is easily modeled using known phonon frequencies in a generalized Lyddane-Sachs-Teller relation.<sup>58</sup> Since these effects are left out of the present calculation we consider

TABLE I. The static electronic ( $\epsilon_\infty$ ) dielectric constants of trigonal selenium and  $\alpha$ -quartz.  $\epsilon_o$  is the ordinary dielectric constant (polarization in the basal plane) and  $\epsilon_e$  is the extraordinary one (polarization along the optic axis). “Scissors” stands for the calculations with the scissors operator and “long” indicates the long-wavelength approximation (i.e., neglect of local fields). The column “Lattice constant” specifies if the lattice constants which minimize the LDA total energy or the experimental lattice constants are used in the calculation. We have used 144  $\mathbf{k}$  points in selenium and 18  $\mathbf{k}$  points in  $\alpha$ -quartz to sample  $\frac{1}{4}$  of the Brillouin zone. The parameter  $\Delta$  in the scissors operator is 1.1 eV for Se and 1.8 eV for  $\alpha$ -quartz.

	Lattice constant	Se		$\alpha$ -quartz	
		$\epsilon_o$	$\epsilon_e$	$\epsilon_o$	$\epsilon_e$
LDA <sup>a</sup>	LDA min.			2.53	2.57
Scissors <sup>a</sup>	LDA min.			2.35	2.39
LDA, long <sup>b</sup>	Expt.			2.86	2.91
LDA, long	Expt.	11.8	16.4	2.61	2.63
LDA	Expt.	10.3	15.2	2.48	2.51
Scissors, long	Expt.	9.0	12.3	2.42	2.43
Scissors	Expt.	7.9	11.5	2.30	2.33
Expt.	Expt.	6.2–8.4 <sup>c</sup>	10.2–13.7 <sup>c</sup>	2.35 <sup>d</sup>	2.38 <sup>d</sup>

<sup>a</sup>Reference 51.

<sup>b</sup>Reference 18.

<sup>c</sup>Reference 72.

<sup>d</sup>Data from Ref. 57 extrapolated to zero frequency.

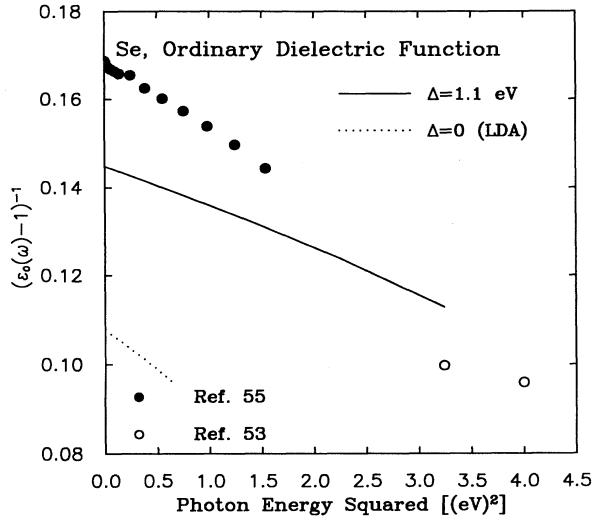


FIG. 1. The frequency-dependent ordinary electronic dielectric function of trigonal selenium (lines) and experiment (dots) (ordinary refers to polarization of the electric field in the basal plane). A linear relationship between  $(\epsilon_o - 1)^{-1}$  and the photon energy squared  $\omega^2$  is predicted by the single-oscillator model (Ref. 10). The plane-wave kinetic-energy cutoff is 10 hartree and 144  $k$  points are used to sample  $\frac{1}{4}$  of the Brillouin zone.

them no further. The agreement between the experimental data and the LDA calculations with scissors correction are within 5% for photon energies well below the gap for all the materials we have studied.

We have also calculated the second-harmonic susceptibility  $d_{11}$  in the static limit. As mentioned earlier, there is another independent component  $d_{14}$  in the second-harmonic tensor. Due to the fact that the scalar-potential perturbation theory can only calculate certain

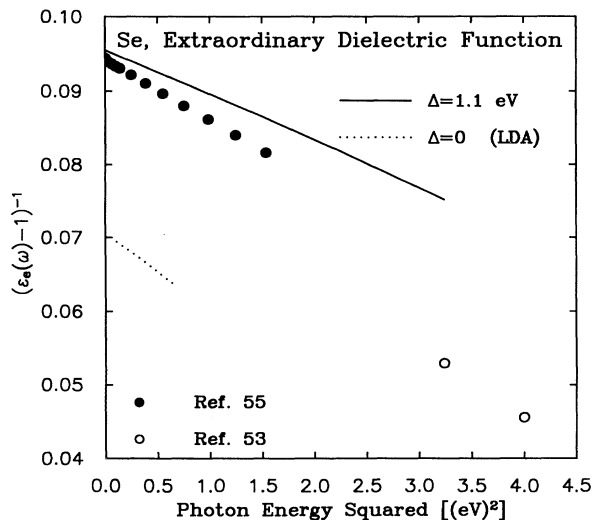


FIG. 2. The frequency-dependent extraordinary electronic dielectric function of trigonal selenium (lines) and experiment (dots) (extraordinary refers to polarization of the electric field along the optic axis). Same convergence parameters as in Fig. 1.

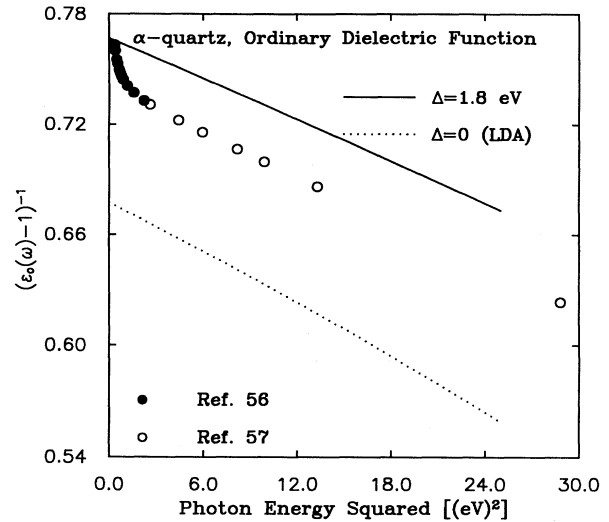


FIG. 3. The frequency-dependent ordinary electronic dielectric function of  $\alpha$ -quartz (lines) and experiment (dots). The plane-wave kinetic-energy cutoff is 23 hartree and 18  $k$  points are used to sample the Brillouin zone.

linear combinations of second-harmonic susceptibilities,<sup>59</sup>  $d_{14}$  cannot be determined within our formalism. Our calculations of  $d_{11}$  for selenium and  $\alpha$ -quartz are summarized in Table II. As shown in the table, our LDA calculation with the self-energy correction for selenium agrees with two of the four experiments. The huge discrepancy of Sherman and Coleman's data is possibly due to the presence of a lattice resonance near  $28 \mu\text{m}$  as they suggested.<sup>60</sup> For  $\alpha$ -quartz, our calculation with the scissors operator agrees with all three experiments. Also for both materials, our results are in fair agreement with the estimates from Levine's bond charge model.<sup>61</sup> Without the scissors operator, LDA overestimates the

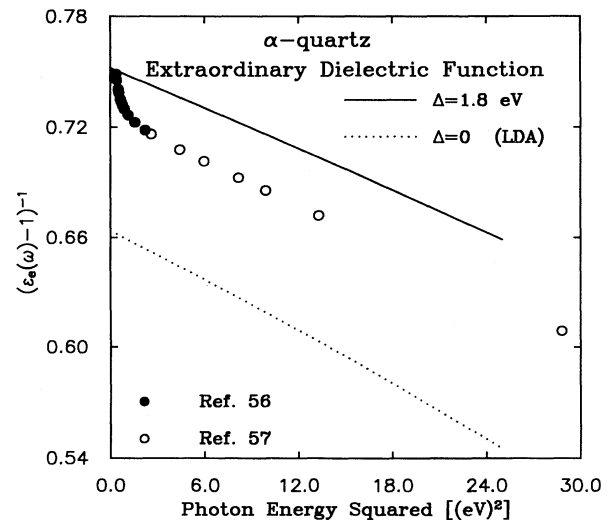


FIG. 4. The frequency-dependent extraordinary electronic dielectric function of  $\alpha$ -quartz (line) and experiment (dots). Same convergence parameters as in Fig. 3.

TABLE II. The static second-harmonic susceptibilities  $d_{11} = \frac{1}{2}\chi_{111}^{(2)}$  of trigonal selenium and  $\alpha$ -quartz. The designation  $d_{11}^{\text{long}}$  is for calculations neglecting local-field corrections. Experimental lattice constants are used.

	$\lambda$ ( $\mu\text{m}$ )	Se		$\alpha$ -quartz	
		$d_{11}^{\text{long}}$ (pm/V)	$d_{11}$ (pm/V)	$d_{11}^{\text{long}}$ (pm/V)	$d_{11}$ (pm/V)
Bond charge model <sup>a</sup>	$\infty$		80		0.33
LDA	$\infty$	179	220	0.507	0.479
Scissors	$\infty$	78	97	0.349	0.330
Expt. <sup>b</sup>	10.6		210 $\pm$ 42		
Expt. <sup>c</sup>	10.64		97 $\pm$ 25		
Expt. <sup>d</sup>	10.6		80 $\pm$ 42		
Expt. <sup>e</sup>	28		1840 $\pm$ 880		
Expt. <sup>f</sup>	1.06				0.335
Expt. <sup>g</sup>	1.0582				0.34 $\pm$ 0.016
Expt. <sup>h</sup>	1.064				0.32 $\pm$ 0.04

<sup>a</sup>Reference 61.

<sup>b</sup>Reference 73.

<sup>c</sup>Reference 64.

<sup>d</sup>Reference 74.

<sup>e</sup>Reference 60.

<sup>f</sup>Reference 75.

<sup>g</sup>Reference 76.

<sup>h</sup>Reference 77.

second-harmonic susceptibilities by 127% for selenium and by 45% for  $\alpha$ -quartz.

Table III shows the contributions to  $d_{11}$  from long-wavelength contribution and local-field corrections. The column  $\phi^0$  is the long-wavelength limit;  $\phi^1$  and  $\phi^2$  are local-field correction terms of first and second order, respectively, in the local-field strength.<sup>21,22</sup> The notations  $ccv$ ,  $vcv$ , and  $cv$  have been explained earlier in the text. We find long-wavelength contribution from  $ccv$  terms dominate in both materials, which is consistent with what was found in other III-V materials.<sup>22</sup> The local-field con-

TABLE III. The terms contributing to the nonlinear susceptibility for second-harmonic generation (in pm/V) in selenium and  $\alpha$ -quartz. The notation  $cv$ ,  $ccv$ , and  $vcv$  follows Aspnes (Ref. 44) convention and is defined in the text. As defined in Refs. 21 and 22,  $\phi^0$  is the long-wavelength limit for the second-harmonic susceptibilities;  $\phi^1$  and  $\phi^2$  are local-field corrections of first and second order, respectively, in the local-field strength. For selenium the plane-wave kinetic-energy cutoff is 10 hartree, the Brillouin-zone integration grid is 144  $\mathbf{k}$  points in  $\frac{1}{4}$  of the Brillouin zone, and the scissors operator  $\Delta$  is 1.1 eV. For  $\alpha$ -quartz the cutoff is 23 hartree, 18  $\mathbf{k}$  points in the Brillouin zone, and the scissors  $\Delta$  is 1.8 eV. The sum rule for the second-harmonic generation, Eq. (13) of Ref. 22, is also listed.

	$\phi^0$	$\phi^1$	$\phi^2$	$d = \frac{1}{2}\chi^{(2)}$	$\Sigma$
Se					
$cv$	0.46	0.02	0	0.48	0.000
$ccv$	77.33	11.04	-0.77	87.60	0.017
$vcv$	2.51	5.93	0.88	9.33	-0.017
total	80.30	16.99	0.11	97.41	0.000
$\alpha$ -quartz					
$cv$	0.008	0.001	0	0.009	0.000 13
$ccv$	0.272	0.063	0.002	0.338	0.000 68
$vcv$	0.068	-0.078	-0.008	-0.017	-0.000 88
total	0.349	-0.013	-0.005	0.330	-0.000 06

tribution is +17% for selenium and -5% for  $\alpha$ -quartz. Selenium is the only example of a material with a positive local-field correction for the second-harmonic susceptibility among the six materials considered to date (i.e., selenium,  $\alpha$ -quartz, and four III-V compounds<sup>21,22</sup>). This may be contrasted with the situation for the dielectric constant, for which the local-field correction in random-phase approximation must always be negative and in LDA is negative under fairly general conditions.<sup>62</sup>

We studied the  $\mathbf{k}$ -point convergence of the linear and nonlinear optical response functions and also their sum rules for selenium. The results are summarized in Table IV, which shows that with 46  $\mathbf{k}$  points, both linear and second-harmonic susceptibilities are converged at the level of a few percent. From Tables I and II, one can see that, although selenium and  $\alpha$ -quartz belong to the same symmetry point group, selenium has a much larger dielectric constant and second-harmonic susceptibilities, consistent with its smaller energy band gap.

TABLE IV. A study of convergence as a function of the number of  $\mathbf{k}$  points of the dielectric function and nonlinear susceptibility for second-harmonic generation for trigonal selenium. The plane-wave kinetic-energy cutoff is 10 hartree. Only the LDA results in the static limit  $\omega=0$  are reported in the table. Sum rules for the linear response and nonlinear susceptibility for second-harmonic generation are represented by  $\Sigma_{\text{linear}}$  and  $\Sigma_{\text{SHG}}$ , which correspond to Eq. (3.37) and Eq. (13) of Ref. 22. Also  $\epsilon_o$  and  $\epsilon_e$  are the ordinary and extraordinary dielectric functions;  $d_{11}$  is the nonlinear susceptibility for second-harmonic generation.

	46	144
$\Sigma_{\text{linear}}$	1.1%	1.0%
$\Sigma_{\text{SHG}}$	0.2%	0.0%
$\epsilon_o$	10.5	10.3
$\epsilon_e$	14.9	15.2
$d_{11}$ (pm/V)	222	220

### B. Optical activity

We apply the formulas derived in Sec. III in the calculations of the optical-activity tensor for trigonal selenium and  $\alpha$ -quartz. With the optical-activity tensor we are able to determine the optical rotatory power along the optic axis and the other independent gyration tensor component  $g_{11}$ , as shown in Eqs. (2.3) and (2.12).

At optical frequencies below the absorption edge, the linear dielectric function  $\epsilon(\omega)$  can be described<sup>10</sup> by the single-oscillator model,

$$\epsilon(\omega) - 1 = \frac{f}{\omega_0^2 - \omega^2}. \quad (4.1)$$

Similarly, the frequency-dependent optical rotatory power of a large variety of optically active crystals can be described by the coupled-oscillator model<sup>4,9</sup>

$$\rho(\omega) = \frac{k\omega^2}{(\omega_0^2 - \omega^2)^2}. \quad (4.2)$$

Experimental data show that for a given crystal the parameter  $k$  is a constant over a wide frequency range. Also for different crystals, the magnitude of  $\rho(\omega)$  can differ by three orders of magnitude while  $k$  varies over only one order of magnitude for 20 different materials.<sup>4</sup> We use the coupled-oscillator model to analyze the experimental and computational results.

We first consider results for the optical rotatory power  $\rho$  for trigonal selenium. Using the space group  $P3_221$ , our calculation constitutes a prediction of the sign of  $\rho$ , which agrees with experiment (positive).<sup>50</sup> Our result in the low-frequency range is about a factor of 2 too low compared with the data of Adams and Haas<sup>63</sup> and one of two points measured by Day<sup>64</sup> as shown in Fig. 5. For frequencies small compared to the band gap,  $(\omega/\omega_{\text{gap}})^2 \ll 1$ , Eq. (1.2) suggests  $\rho \propto \omega^2$ . Our calculated results with the scissors correction are consistent with  $\rho \propto \omega^{1.9}$ . The data of Day, however, are fitted to  $\rho \propto \omega^{0.6 \pm 0.3}$ , which is inconsistent with the coupled-oscillator model. There is a large discrepancy between the Adams-Haas and the Henrion-Eckart<sup>50</sup> data sets. The Adams-Haas data show a kink near  $\omega = 1.3$  eV which is not consistent with the coupled-oscillator model; the data of Henrion and Eckart shows no such kink. It is our opinion that the kink is unlikely to be a real feature; however, our calculation does not probe the frequencies of the kink because the accuracy of the Brillouin-zone integrations we can afford becomes progressively worse as we approach the gap energy, as discussed below. The other independent gyration component of selenium ( $g_{11}$ ) is shown in Fig. 6; there is apparently no experimental data for comparison. We obtain a negative  $g_{11}$  for selenium as for  $\alpha$ -quartz, but the ratio  $g_{11}/g_{33}$  is not close to  $-0.5$  as for  $\alpha$ -quartz (see discussion below). We have modified our results from those reported earlier due to the discovery of errors and published an erratum to this effect.<sup>1</sup>

Up to 1.05 eV, our selenium results (cf. Table V) for the 144 and 410  $k$  points are within 20% agreement. However, at higher frequencies, this agreement breaks down. Because the integrand becomes singular at the

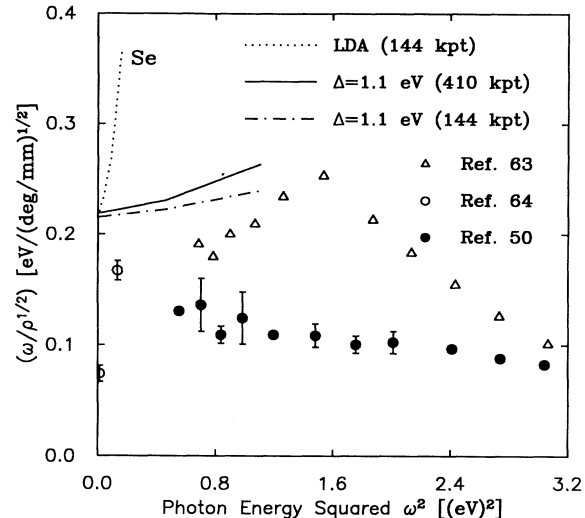


FIG. 5. Frequency dependence of the optical rotatory power  $\rho(\omega)$  for selenium. We plot  $\omega/\rho^{1/2}$  as a function of the photon frequency squared  $\omega^2$ , which should be a straight line according to the coupled-oscillator model (Refs. 8 and 9). The model should begin to fail at frequencies close to the absorption edge. We display the LDA result for 144  $k$  points in  $\frac{1}{4}$  of the Brillouin zone (dotted line) and the self-energy-corrected result with  $\Delta = 1.1$  eV for 144 (dash-dotted line) and 410 (solid line)  $k$  points.

band gap, our uniform sampling method must fail at some frequency. In Table V we show the convergence study of the sum rule  $S$  for optical activity and the rotatory power  $\rho(\omega)$  of trigonal selenium as we vary the number of  $k$  points to sample the Brillouin zone.

In order to save computation time, we have set an

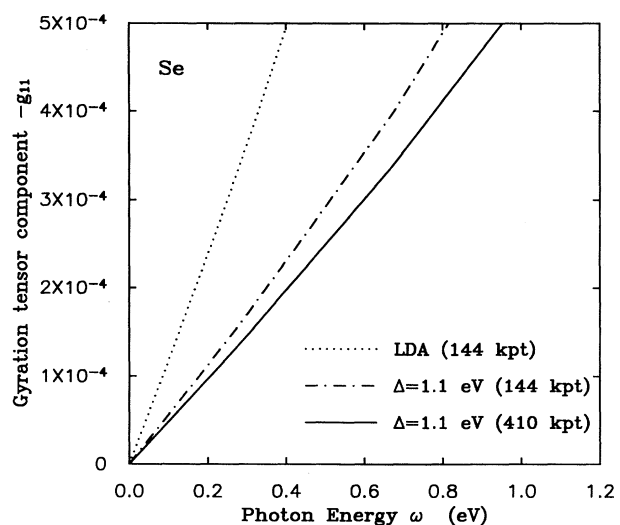


FIG. 6. The gyration tensor component  $g_{11} = q\eta_{312}$  for selenium. For the trigonal point group,  $\eta_{312}$  is the only independent tensor component other than  $\eta_{231}$  (which was used to determine the optical rotatory power in Fig. 5).

TABLE V. A study of convergence as a function of the number of  $\mathbf{k}$  points of the optical activity sum rule and the optical rotatory power of selenium. The  $\mathbf{k}$  points indicated in the table are in  $\frac{1}{4}$  of the Brillouin zone. (We did not invoke the nonsym-morphic symmetry operators.) The sum rule for the optical activity is evaluated using  $S_{ijl}$  defined in Eq. (3.51). The subscript indicates the Cartesian components. The table shows that for frequencies higher than 1.05 eV, the uniform sampling of the  $\mathbf{k}$  point scheme fails to give a well-converged value for the optical rotatory power.

	$\omega$ (eV)	Number of $\mathbf{k}$ points		
		46	144	410
$S_{231}$	0	0.031	0.029	0.016
$S_{321}$	0	0.069	0.069	0.011
$\rho(\omega)$ (deg/mm)	0.1	0.35	0.22	0.21
	0.3	3.17	1.92	1.85
	0.675	16.42	9.20	8.57
	1.05	41.71	19.18	15.88
	1.425	84.65	21.73	5.79

upper limit for the eigenenergies involved in the spectral sum. The contributions to the sum rule, Eq. (3.38), or the optical activity tensor, Eq. (3.43), from the conduction-band Green function when  $\epsilon_{mk} \gg \epsilon_{nk}$  are minimal. We set  $E_{\text{cut}}^{(sp)}$  to be the highest energy eigenvalues included in the spectral sum such that

$$G_{nk}^c = \sum_{m \in c}^{\epsilon_{mk} \leq E_{\text{cut}}^{(sp)}} \frac{|m\mathbf{k}\rangle\langle m\mathbf{k}|}{\epsilon_{nk} - \epsilon_{mk}} \quad (4.3)$$

in the computation. Table VI shows the  $E_{\text{cut}}^{(sp)}$  convergence study of the optical rotatory power  $\rho(\omega)$ . As shown in the table, with about 150 bands included in the spectral sum for selenium, one can expect a converged value for the optical activity tensor within an accuracy of 2%. The convergence study for  $\alpha$ -quartz is presented in Table VII for various optical response functions, which illustrates a lower accuracy is achieved with 200 bands

TABLE VI. A convergence study of the optical rotatory power of selenium as a function of  $E_{\text{cut}}^{(sp)}$ . To save computation time, a parameter  $E_{\text{cut}}^{(sp)}$  is set to be the highest eigenvalue included in the spectral sum so that terms with small contributions are not included in the computation. For  $E_{\text{cut}}^{(sp)} = 2, 3,$  and 5 hartree listed in the table, the corresponding total number of (valence and conduction) bands are 76, 140, and 300, respectively. Results shown in the table are computed with plane-wave kinetic-energy cutoff  $E_{\text{cut}} = 10$  hartree, 144  $\mathbf{k}$  points, and  $\Delta = 1.1$  eV. At different frequencies and  $E_{\text{cut}}^{(sp)}$  values, the optical rotatory power  $\rho(\omega)$  are listed in the table.

$\omega$ (eV)	$E_{\text{cut}}^{(sp)}$ (hartree)	$\rho$ (deg/mm)		
		2	3	5
0.1		0.208	0.213	0.215
0.3		1.850	1.893	1.919
0.675		8.843	9.069	9.203
1.05		18.265	18.842	19.181

TABLE VII. The  $E_{\text{cut}}^{(sp)}$  convergence study for  $\alpha$ -quartz. The plane-wave kinetic-energy cutoff for the ground-state calculation is 23 hartree and 18  $\mathbf{k}$  points are used to sample the Brillouin zone. For  $E_{\text{cut}}^{(sp)} = 3$  and 5 hartree, the equivalent total number of the (valence and conduction) bands in the spectral sum are 200 and 400, respectively. Sum rules for the linear response, second-harmonic generation, and both components of the optical activity tensor are represented by  $\Sigma_{\text{linear}}, \Sigma_{\text{SHG}}, \Sigma_{231},$  and  $\Sigma_{321}$ , respectively. When labeled "Scissors," a self-energy correction of 1.8 eV is implied. Symbols for the optical response functions are defined in the text.

	$\omega$ (eV)	$E_{\text{cut}}^{(sp)}$ (hartree)	
		3	5
$\Sigma_{\text{linear}}$	0	13%	5.2%
$\Sigma_{\text{SHG}}$	0	9%	3.5%
$\Sigma_{231}$	0	39%	0.5%
$\Sigma_{321}$	0	33%	5.3%
LDA $\epsilon_o$	0	2.47	2.48
LDA $\epsilon_e$	0	2.51	2.51
LDA $d_{11}$ (pm/V)	0	0.467	0.479
Scissors $\eta_{231} 10^{-3}$ ( $\text{\AA}$ )	1	0.941	1.015
Scissors $\eta_{321} 10^{-3}$ ( $\text{\AA}$ )	1	0.404	0.473

included.

To analyze the contributions to the optical-activity tensor and the sum rule, we have separately listed the  $cv, ccv,$  and  $vvc$  terms computed from Eqs. (3.52)–(3.54) and Eqs. (3.47)–(3.49) in Table VIII. Comparing with the second-harmonic susceptibilities listed in Table III, we found the contributions from the  $vvc$  terms are large and can exceed 50% of the  $ccv$  terms in the optical-activity tensor. For the sum rule, in selenium the cancellation is between the  $ccv$  and  $vvc$  terms; in  $\alpha$ -quartz, the cancellation is between the  $ccv + vvc$  terms and the  $cv$  term.

TABLE VIII. The terms contributing to both of the optical activity tensor components  $\eta_{231}$  and  $\eta_{321}$  (in units of  $10^{-3} \text{\AA}$ ) in selenium and  $\alpha$ -quartz. The symbols  $cv, ccv,$  and  $vvc$  are defined in the text. Numerical results are obtained with 10 hartree cutoff energy, 144  $\mathbf{k}$  points, and the self-energy correction  $\Delta = 1.1$  eV for selenium; 23 hartree, 18  $\mathbf{k}$  points, and  $\Delta = 1.8$  eV for  $\alpha$ -quartz. The sum rules are examined at  $\omega = 0$  and  $\Delta = 0$  for both cases.

	Se $\omega = 0.3$ eV		$\alpha$ -quartz $\omega = 1$ eV	
	$\eta_{231}$	$\eta_{321}$	$\eta_{231}$	$\eta_{321}$
$cv$	-0.074	-0.037	-0.137	-0.069
$ccv$	75.023	50.720	0.709	0.340
$vvc$	-45.963	-11.076	0.443	0.201
total	28.986	39.606	1.015	0.473
	$\omega = 0$		$\omega = 0$	
	$\Sigma_{231}$	$\Sigma_{321}$	$\Sigma_{231}$	$\Sigma_{321}$
$cv$	0.015	0.008	-0.019	-0.009
$ccv$	0.407	0.170	0.010	0.004
$vvc$	-0.398	-0.205	0.008	0.004
total	0.024	-0.027	$-10^{-4}$	-0.001

Figure 7 shows the computed optical rotatory power of  $\alpha$ -quartz. As suggested by the coupled-oscillator model Eq. (1.2),  $\omega/\rho^{1/2}$  depends linearly on the square of the photon energy  $\omega^2$ . Our theoretical results, with or without the self-energy corrections, and the experimental data (except for the lowest-frequency data point) agree well with the model. Our theoretical predictions for the parameter  $k$  in Eq. (1.2), the slopes of the lines in Fig. 7, are  $-0.052$  and  $-0.047$  with and without the scissors operator, respectively; the corresponding experimental data suggest  $-0.049$ . This calculation also identifies the space group  $P3_221$  with right-handed quartz (positive rotatory power) in agreement with experiment.<sup>5,12,32</sup> However, our theoretical calculation of the magnitude of the optical rotatory power is about a factor of 5 too small compared with the experimental value.

We also calculated  $g_{11}$  for  $\alpha$ -quartz, which is plotted in Fig. 8. Our theoretical results show that  $g_{11}$  is negative, consistent with experiment.<sup>27,32</sup> Like our value for  $\rho$ , our value for  $g_{11}$  is much smaller than that seen experimentally. Experiments measured the ratio of the two independent gyration tensor components  $g_{11}/g_{33}$  to be  $-0.45$  (Ref. 32) or  $-0.53$  (Ref. 65), independent of photon frequency. In the nonabsorptive regime this should be  $-0.5$  according to a symmetry argument.<sup>4</sup> This argument states that quartz is made up of  $\text{SiO}_4$  tetrahedron "building units." These tetrahedra locally possess a mirror plane symmetry which causes the pseudoscalar part of the gyration tensor to vanish, giving  $g_{33} + 2g_{11} = 0$  [Eq. (30) of Ref. 4]. The argument does not apply equally well to trigonal selenium because the building units here

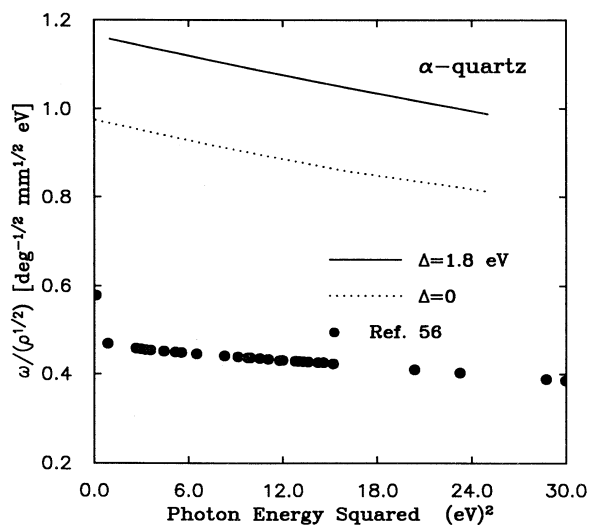


FIG. 7. Frequency dependence of the optical rotatory power  $\rho(\omega)$  for  $\alpha$ -quartz, plotted as in Fig. 5. Computational results both with and without the scissors correction obey the coupled-oscillator model. Except for one data point at very low frequency, experimental data also suggest a linear relation between  $\omega/\rho^{1/2}$  and  $\omega^2$ . The slopes of both theoretical lines agree with the experiment's within 10%. However, our computation results for  $\rho(\omega)$  are about factor of 5 too low compared with the experiment.

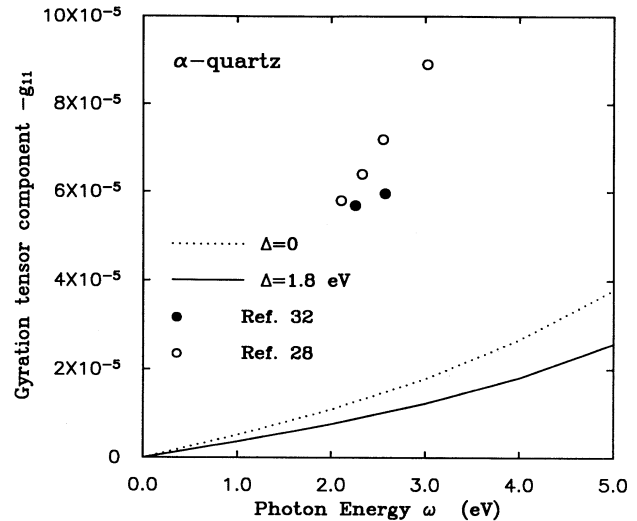


FIG. 8. The gyration tensor component  $g_{11}$  of  $\alpha$ -quartz. We obtain the experimentally observed sign for  $g_{11}$  (negative). The magnitude of our theoretical results are about five times smaller than the available experimental data of Refs. 28 and 32. We use 18 special  $k$  points to sample a quarter of the Brillouin zone and 23 hartree for the plane-wave kinetic-energy cutoff for calculations both with and without the scissors correction.

would have to be chains of selenium atoms which possess no higher symmetry than the space group, i.e., no local mirror symmetry. Our computational result for  $g_{11}/g_{33}$  for quartz is  $-0.46$ , consistent with the symmetry argument, in spite of the fact that each value is smaller than that seen in experiment. Our computational result for  $g_{11}/g_{33}$  for selenium is close to  $-1.0$  at low frequencies.

To summarize, we obtain good agreement for the dielectric functions and the second-harmonic susceptibilities for both selenium and  $\alpha$ -quartz. For optical rotatory power, our theoretical results for selenium are about factor of 2 too small compared with some of the experimental data in the low-frequency range; for  $\alpha$ -quartz, it is factor of 5 too low. Our calculated results are apparently converged, given that the sum rule for the optical activity tensor for  $\alpha$ -quartz is within 5% of the theoretical ideal value.

The formulas presented in Sec. III are obtained in the long-wavelength limit, i.e., local-field corrections are not included. We found the local-field contributions for the dielectric functions and second-harmonic susceptibilities are  $-5\%$  and  $+17\%$  for  $\alpha$ -quartz and selenium, respectively. It is possible that the local-field corrections are much larger for optical activity. One paper suggests that local-field effects should be greatly enhanced in optical activity over linear susceptibility.<sup>4</sup>

Our calculations use the frozen-ion approximation, in which motions of the ionic lattice are ignored. There are theories which argue that the phonon excitations and electron-phonon interactions play an important role in optical activity.<sup>66,67</sup> Within the electronic optical-activity theory itself, we have ignored excitonic effects and spin-orbit interactions, and self-energy effects are

considered only at the scissors operator level with constant energy shift.

Looking back over experimental work, for many years quartz was the only material for which the theory of optical activity of Ewald and Born from the 1910s and 1920s had been verified. The experiments of Voigt<sup>68</sup> of 1905 were confirmed by Wever in 1920,<sup>69</sup> but contested by Szivessy and Schweers in 1929.<sup>70</sup> This controversy, and the desire to verify the theory of optical activity in crystals, lead to new measurements by Szivessy and Münster<sup>65</sup> in 1934 and Bruhat and Grivet in 1935.<sup>71</sup> These experiments were quite different, that of Szivessy and Münster using visible light, with the direction of propagation within 25° of the optic axis, whereas Bruhat and Grivet used ultraviolet light and measured parallel and perpendicular to the optic axis using some six different methods. Plate thicknesses were varied systematically over an order of magnitude and both left- and right-handed crystals were studied. Both of these works confirmed the work of Voigt and Wever and discussed the artifacts and errors of the Szivessy and Schweers study.

More recently, Konstantinova, Ivanov, and Grechushnikov<sup>32</sup> were motivated to return to the optics of quartz to verify the details of a theory proposed by Federov. They confirmed the earlier work as did Kobayashi *et al.*,<sup>28</sup> who were motivated to return to the optics of quartz to verify a new method for measuring the optical gyration tensor as part of an effort to understand optical activity in ferroelectric crystals. We use the word “confirmed” in the sense of agreement to within about 20%. This is reasonable agreement for a difficult measurement from six laboratories in four countries and spread across eight decades. A more refined study of the experiments would be required to choose a preferred value within this range.

## V. SUMMARY

We have derived a band-theoretic formula to calculate the optical-activity tensor from vector-potential perturbation theory. It is necessary to compute the induced-current density in response to a vector-potential perturbation, instead of studying the induced charge density in response to a scalar-potential perturbation which some of us have used previously for other properties. Using the formula obtained from the microscopic theory, we prove that the optical activity tensor has the desired macroscopic symmetry. With the sum rules, which we verify numerically, we obtain formulas for the dielectric constants and optical activity tensor which have well-defined values in the static limit. To eliminate possible numerical difficulties, the contributions to the optical-activity tensor are divided into valence and conduction parts.

We have calculated the optical rotatory power along the optic axis and the other independent gyration tensor component  $g_{11}$  for both trigonal selenium and  $\alpha$ -quartz as well as linear dielectric response and the second-harmonic susceptibility. Our calculations are performed directly from nearly first-principles band-structure calculations. The experimental input is limited to the dimen-

sions of the unit cell and self-energy corrections to the band gap. We are able to obtain the correct signs for the optical rotatory power and  $g_{11}$  for both materials. Our calculations for the optical rotatory power for selenium are nearly a factor of 2 too small compared with some of the experimental data. For  $\alpha$ -quartz, we obtain good agreement with the experiments for the dispersion constant  $k$  in the coupled-oscillator model and the ratio of  $g_{11}/g_{33}$ , consistent with arguments from symmetry, yet the magnitudes of both  $g_{11}$  and  $g_{33}$  are about factor of 5 too small. The possible reasons for the discrepancy are the local-field corrections, electron and phonon excitations and their interactions, and other effects. The fact that we can account for both the linear and second-harmonic optical properties as well as satisfying several sum rules limits the scope for the origin of the discrepancy.

## ACKNOWLEDGMENTS

This work was supported by the DOE–Basic Energy Sciences, Division of Material Sciences and the Ohio Supercomputer Center. We thank Xavier Gonze, Lars Jönsson, Jay Lawrence, and Robert Mills for helpful discussions, and Michael Teter for assistance in preparing the pseudopotentials.

## APPENDIX A: PERTURBATION IN PRESENCE OF A NONLOCAL POTENTIAL

In general, the potentials considered in a Hamiltonian may be nonlocal. Norm-conserving nonlocal pseudopotential are used in our calculation; the approximation to the electron self-energy is also nonlocal.

In the presence of a nonlocal potential  $V^{nl}(\mathbf{r}, \mathbf{r}')$ , the Schrödinger equation is not gauge invariant.<sup>78</sup> Equally unpleasant, the Schrödinger equation with a nonlocal potential, even in the absence of an electromagnetic field, *does not* lead to the form of the charge current as  $\mathbf{J}(\mathbf{r}, t) = -(i/2)[\psi(\mathbf{r}, t)\nabla_{\mathbf{r}}\psi^*(\mathbf{r}, t) - \psi^*(\mathbf{r}, t)\nabla_{\mathbf{r}}\psi(\mathbf{r}, t)]$  satisfying the continuity relation

$$\nabla_{\mathbf{r}} \cdot \mathbf{J}(\mathbf{r}, t) + \frac{\partial \rho(\mathbf{r}, t)}{\partial t} = 0. \quad (\text{A1})$$

Yet the continuity relation must be satisfied so that the Maxwell equations, which are consistent with the continuity relation, are preserved.

To solve the problems discussed above, one needs to modify the expression for the current density to take into account the effects of a nonlocal potential. With the unperturbed nonlocal Hamiltonian,  $\hat{H} = \frac{1}{2}\hat{\mathbf{p}}^2 + \hat{V} + \hat{V}^{nl}$ , the velocity operator is  $\hat{v}^{(0)} \equiv (-i)[\hat{\mathbf{p}}, \hat{H}] = \hat{\mathbf{p}} + (-i)[\hat{\mathbf{p}}, \hat{V}^{nl}]$ , where we have used the fundamental definition for the velocity<sup>79</sup> and  $\hat{\mathbf{p}}$  and  $\hat{V}^{nl}$  *do not* commute.

In the coordinate representation, the velocity operator can be written as

$$\hat{v}^{(0)}(\mathbf{r}, \mathbf{r}') = -i\nabla_{\mathbf{r}}\delta(\mathbf{r} - \mathbf{r}') - i(\mathbf{r} - \mathbf{r}')\hat{V}^{nl}(\mathbf{r}, \mathbf{r}'). \quad (\text{A2})$$

With Eq. (A2), the current at position  $\mathbf{R}$  in the coordinate representation  $\hat{\mathbf{J}}^{(0)}(\mathbf{R}, \mathbf{r}, \mathbf{r}')$  can be written<sup>39</sup> as

$$\begin{aligned} \hat{J}^{(0)}(\mathbf{R}, \mathbf{r}, \mathbf{r}') &= \frac{i}{2} [\nabla_{\mathbf{r}} \delta(\mathbf{r} - \mathbf{r}') \delta(\mathbf{r} - \mathbf{R}) \\ &\quad + \delta(\mathbf{r} - \mathbf{R}) \nabla_{\mathbf{r}} \delta(\mathbf{r} - \mathbf{r}')] \\ &\quad + \frac{i}{2} (\mathbf{r} - \mathbf{r}') \hat{V}^{nl}(\mathbf{r}, \mathbf{r}') \\ &\quad \times [\delta(\mathbf{r}' - \mathbf{R}) + \delta(\mathbf{r} - \mathbf{R})]. \end{aligned} \quad (\text{A3})$$

The symmetric combinations are used to form the nonlocal current, which is necessary to make  $\hat{J}^{(0)}(\mathbf{R}, \mathbf{r}, \mathbf{r}')$  a Hermitian operator. We use this current operator to obtain an expression for the perturbed Hamiltonian in the presence of a nonlocal potential.

A general expression for the first-order perturbation<sup>39</sup> is

$$\hat{H}^{(1)}(t) = -\alpha \int d\mathbf{R} \hat{J}^{(0)}(\mathbf{R}) \cdot \mathbf{A}(\mathbf{R}, t), \quad (\text{A4})$$

where the superscript indicates the order of  $\mathbf{A}$ . In the coordinate representation, the first-order perturbation is

$$\begin{aligned} \frac{i}{2} \alpha V^{nl}(\mathbf{r}, \mathbf{r}') (\mathbf{r}' - \mathbf{r}) \cdot \mathbf{A}_{\mathbf{q}} e^{i(\mathbf{q} \cdot \mathbf{r}' - \omega t)} &= \frac{i}{2} \alpha V^{nl}(\mathbf{r}, \mathbf{r}') (\mathbf{r}' - \mathbf{r}) \cdot \mathbf{A}(\mathbf{r}, t) e^{i\mathbf{q} \cdot (\mathbf{r}' - \mathbf{r})} \\ &= \frac{i}{2} \alpha V^{nl}(\mathbf{r}, \mathbf{r}') (\mathbf{r}' - \mathbf{r}) \cdot \mathbf{A}(\mathbf{r}, t) - \frac{\alpha}{2} V^{nl}(\mathbf{r}, \mathbf{r}') [(\mathbf{r}' - \mathbf{r}) \cdot \mathbf{A}(\mathbf{r}, t)] [(\mathbf{r}' - \mathbf{r}) \cdot \mathbf{q}] + O(q^2). \end{aligned} \quad (\text{A8})$$

Combining Eqs. (A6) and (A8), we obtain

$$\begin{aligned} \hat{H}^{(1)}(\mathbf{r}, \mathbf{r}', t) &= -\frac{i}{2} \alpha [\nabla_{\mathbf{r}} \cdot \mathbf{A}(\mathbf{r}, t) \delta(\mathbf{r} - \mathbf{r}') + \mathbf{A}(\mathbf{r}, t) \cdot \nabla_{\mathbf{r}} \delta(\mathbf{r} - \mathbf{r}')] \\ &\quad + i\alpha (\mathbf{r}' - \mathbf{r}) \cdot \mathbf{A}(\mathbf{r}, t) V^{nl}(\mathbf{r}, \mathbf{r}') - \frac{\alpha}{2} [(\mathbf{r}' - \mathbf{r}) \cdot \mathbf{A}(\mathbf{r}, t)] [(\mathbf{r}' - \mathbf{r}) \cdot \mathbf{q}] V^{nl}(\mathbf{r}, \mathbf{r}') + O(q^2). \end{aligned} \quad (\text{A9})$$

The same expression for the perturbed Hamiltonian in the presence of a nonlocal potential may be obtained with Korolev's approach.<sup>80</sup> The unperturbed Schrödinger equation of an electron in a nonlocal potential takes the form

$$-\frac{1}{2} \nabla^2 \psi(\mathbf{r}) + V(\mathbf{r}) \psi(\mathbf{r}) + \int d\mathbf{r}' V^{nl}(\mathbf{r}, \mathbf{r}') \psi(\mathbf{r}') = \epsilon \psi(\mathbf{r}). \quad (\text{A10})$$

Recall that  $e^{(\mathbf{r}' - \mathbf{r}) \cdot \nabla_{\mathbf{r}}}$  is a displacement operator such that  $\psi(\mathbf{r}') = e^{(\mathbf{r}' - \mathbf{r}) \cdot \nabla_{\mathbf{r}}} \psi(\mathbf{r})$  for any function  $\psi(\mathbf{r})$  which has a convergent Taylor series. We can rewrite

$$\begin{aligned} \int d\mathbf{r}' V^{nl}(\mathbf{r}, \mathbf{r}') \psi(\mathbf{r}') &= \int d\mathbf{r}' V^{nl}(\mathbf{r}, \mathbf{r}') e^{i(\mathbf{r}' - \mathbf{r}) \cdot \hat{\mathbf{p}}} \psi(\mathbf{r}) \\ &= V^{nl}(\mathbf{r}, \hat{\mathbf{p}}) \psi(\mathbf{r}), \end{aligned} \quad (\text{A11})$$

where  $\hat{\mathbf{p}} = -i\nabla_{\mathbf{r}}$  is the momentum operator and  $V^{nl}(\mathbf{r}, \hat{\mathbf{p}})$  is implicitly defined. In other words, a nonlocal potential can be rewritten as a function of the momentum operator.

In the presence of an electromagnetic field, the momentum operator  $\hat{\mathbf{p}}$  should be replaced by  $\hat{\pi} = \hat{\mathbf{p}} + \alpha \mathbf{A}(\mathbf{r}, t)$  in the Hamiltonian. (This is often referred to as "minimal coupling" and ensures the gauge invariance of the Schrödinger equation.) The nonlocal potential  $V(\mathbf{r}, \mathbf{r}')$  in Eq. (A11) becomes

$$\hat{H}^{(1)}(\mathbf{r}, \mathbf{r}', t) = -\alpha \int d\mathbf{R} \hat{J}^{(0)}(\mathbf{R}, \mathbf{r}, \mathbf{r}') \cdot \mathbf{A}(\mathbf{R}, t). \quad (\text{A5})$$

Substituting Eq. (A3) in the above expression leads to

$$\begin{aligned} \hat{H}^{(1)}(\mathbf{r}, \mathbf{r}', t) &= -\frac{i}{2} \alpha [\nabla_{\mathbf{r}} \cdot \mathbf{A}(\mathbf{r}, t) \delta(\mathbf{r} - \mathbf{r}') \\ &\quad + \mathbf{A}(\mathbf{r}, t) \cdot \nabla_{\mathbf{r}} \delta(\mathbf{r} - \mathbf{r}')] \\ &\quad + \frac{i}{2} \alpha (\mathbf{r}' - \mathbf{r}) \cdot \mathbf{A}(\mathbf{r}, t) V^{nl}(\mathbf{r}, \mathbf{r}') \\ &\quad + \frac{i}{2} \alpha V^{nl}(\mathbf{r}, \mathbf{r}') (\mathbf{r}' - \mathbf{r}) \cdot \mathbf{A}(\mathbf{r}, t). \end{aligned} \quad (\text{A6})$$

Further, with a monochromatic assumption

$$\mathbf{A}(\mathbf{r}, t) = \mathbf{A}_{\mathbf{q}} e^{i(\mathbf{q} \cdot \mathbf{r} - \omega t)}, \quad (\text{A7})$$

and the Taylor expansion,  $e^{i\mathbf{q} \cdot (\mathbf{r}' - \mathbf{r})} \approx 1 + i\mathbf{q} \cdot (\mathbf{r}' - \mathbf{r})$  to first order in  $\mathbf{q}$ , the last term in Eq. (A6) can be written as

$$\begin{aligned} \int d\mathbf{r}' V^{nl}(\mathbf{r}, \mathbf{r}') e^{i(\mathbf{r}' - \mathbf{r}) \cdot \hat{\pi}} \psi(\mathbf{r}) &= \int d\mathbf{r}' V^{nl}(\mathbf{r}, \mathbf{r}') e^{i(\mathbf{r}' - \mathbf{r}) \cdot \hat{\pi}} e^{-i(\mathbf{r}' - \mathbf{r}) \cdot \hat{\mathbf{p}}} \psi(\mathbf{r}') \\ &= \int d\mathbf{r}' V^{nl}(\mathbf{r}, \mathbf{r}') \hat{\Gamma}(\mathbf{r}' - \mathbf{r}) \psi(\mathbf{r}'), \end{aligned} \quad (\text{A12})$$

where we have defined  $\hat{\Gamma}(\mathbf{r}' - \mathbf{r}) = e^{i(\mathbf{r}' - \mathbf{r}) \cdot \hat{\pi}} e^{-i(\mathbf{r}' - \mathbf{r}) \cdot \hat{\mathbf{p}}}$ . To simplify the notation, we set  $\mathbf{x} = \mathbf{r}' - \mathbf{r} = x \hat{\mathbf{x}}$ ,  $\hat{\pi}_x = \hat{\pi} \cdot \hat{\mathbf{x}}$ , and  $\hat{\mathbf{p}}_x = \hat{\mathbf{p}} \cdot \hat{\mathbf{x}}$ . Therefore we obtain

$$\hat{\Gamma}(x) = e^{ix \hat{\pi}_x} e^{-ix \hat{\mathbf{p}}_x}, \quad (\text{A13})$$

and

$$\begin{aligned} \frac{d\hat{\Gamma}(x)}{dx} &= i e^{ix \hat{\pi}_x} (\hat{\pi}_x - \hat{\mathbf{p}}_x) e^{-ix \hat{\mathbf{p}}_x} \\ &= i \alpha e^{ix \hat{\pi}_x} A_x(\mathbf{r}, t) e^{-ix \hat{\mathbf{p}}_x} \\ &= i \alpha e^{ix \hat{\pi}_x} e^{-ix \hat{\mathbf{p}}_x} e^{ix \hat{\mathbf{p}}_x} A_x(\mathbf{r}, t) e^{-ix \hat{\mathbf{p}}_x} \\ &= i \alpha \hat{\Gamma} e^{ix \hat{\mathbf{p}}_x} A_x(\mathbf{r}, t) e^{-ix \hat{\mathbf{p}}_x}. \end{aligned} \quad (\text{A14})$$

Using the definition of the displacement operator,

$$e^{ix \hat{\mathbf{p}}_x} A_x(\mathbf{r}, t) e^{-ix \hat{\mathbf{p}}_x} = A_x(\mathbf{r} + x \hat{\mathbf{x}}, t). \quad (\text{A15})$$

To first order in  $\mathbf{A}$ , the solution of Eq. (A14) is

$$\hat{\Gamma}(\mathbf{x}) = 1 + i\alpha \int_0^x dx' A_x(\mathbf{r} + x'\hat{\mathbf{x}}, t). \quad (\text{A16})$$

Recall  $\mathbf{x} = \mathbf{r}' - \mathbf{r} = x\hat{\mathbf{x}}$ . The integral indicated in Eq.

(A16), is simply a path integral along a straight line from  $\mathbf{r}$  to  $\mathbf{r}'$  of vector potential  $\mathbf{A}(\mathbf{r}, t)$ .

Using the monochromatic form of Eq. (3.3), the integral in Eq. (A16) can be simplified:

$$\begin{aligned} \Gamma(x) &= 1 + i\alpha \int_0^x dx' A_x(\mathbf{r} + x'\hat{\mathbf{x}}, t) \\ &= 1 + i\alpha \hat{\mathbf{x}} \cdot \mathbf{A}_q e^{i(\mathbf{q}\cdot\mathbf{r} - \omega t)} \int_0^x dx' e^{iq\cdot\hat{\mathbf{x}}x'} \\ &= 1 + i\alpha \hat{\mathbf{x}} \cdot \mathbf{A}_q e^{i(\mathbf{q}\cdot\mathbf{r} - \omega t)} \left[ \frac{e^{iq\cdot\hat{\mathbf{x}}x} - 1}{iq\cdot\hat{\mathbf{x}}} \right] \\ &= 1 + i\alpha \hat{\mathbf{x}} \cdot \mathbf{A}_q e^{i(\mathbf{q}\cdot\mathbf{r} - \omega t)} \left[ x + \frac{i}{2} x^2 \mathbf{q} \cdot \hat{\mathbf{x}} + O(q^2) \right] \\ &= 1 + i\alpha (\mathbf{r}' - \mathbf{r}) \cdot \mathbf{A}(\mathbf{r}, t) - \frac{\alpha}{2} [(\mathbf{r}' - \mathbf{r}) \cdot \mathbf{A}(\mathbf{r}, t)] [(\mathbf{r}' - \mathbf{r}) \cdot \mathbf{q}] + O(q^2), \end{aligned} \quad (\text{A17})$$

where in the long-wavelength limit, we have used the Taylor expansion of  $e^{iq\cdot\hat{\mathbf{x}}x}$ .

With Eqs. (A12) and (A17), we obtain the first-order perturbed Hamiltonian  $\hat{H}^{(1)}$ ,

$$\begin{aligned} \hat{H}^{(1)}(\mathbf{r}, \mathbf{r}', t) &= -\frac{i\alpha}{2} [\nabla_{\mathbf{r}'} \cdot \mathbf{A}(\mathbf{r}, t) \delta(\mathbf{r} - \mathbf{r}') + \mathbf{A}(\mathbf{r}, t) \cdot \nabla_{\mathbf{r}'} \delta(\mathbf{r} - \mathbf{r}')] \\ &\quad + i\alpha (\mathbf{r}' - \mathbf{r}) \cdot \mathbf{A}(\mathbf{r}, t) V^{nl}(\mathbf{r}, \mathbf{r}') - \frac{\alpha}{2} [(\mathbf{r}' - \mathbf{r}) \cdot \mathbf{A}(\mathbf{r}, t)] [(\mathbf{r}' - \mathbf{r}) \cdot \mathbf{q}] V^{nl}(\mathbf{r}, \mathbf{r}') + O(q^2). \end{aligned} \quad (\text{A18})$$

Equation (A18) is the perturbed Hamiltonian we obtained in Eq. (A9).

Following similar procedures, the terms second order in  $\mathbf{A}(\mathbf{r}, t)$  in the Hamiltonian are

$$\begin{aligned} \hat{H}^{(2)}(\mathbf{r}, \mathbf{r}', t) &= \frac{\alpha^2}{2} \delta(\mathbf{r} - \mathbf{r}') \mathbf{A}^2(\mathbf{r}, t) \\ &\quad - \frac{\alpha^2}{2} V^{nl}(\mathbf{r}, \mathbf{r}') [(\mathbf{r}' - \mathbf{r}) \cdot \mathbf{A}(\mathbf{r}, t)] \\ &\quad \times [(\mathbf{r}' - \mathbf{r}) \cdot \mathbf{A}(\mathbf{r}, t)]. \end{aligned} \quad (\text{A19})$$

## APPENDIX B: OPTICAL ACTIVITY TENSOR WITH SCISSORS OPERATOR

The formula for the optical activity tensor has been given in Eqs. (3.51)–(3.54), in which

$$\hat{H}_{\mathbf{k}} = \hat{H}_{\mathbf{k}}^L + \Delta P_{c\mathbf{k}}, \quad (\text{B1})$$

where  $\hat{H}_{\mathbf{k}}^L$  is the LDA Hamiltonian,  $\Delta$  is the energy shift,

and  $P_{c\mathbf{k}}$  is a projection operator onto conduction bands. The implementation of the scissors operator with proper velocity renormalization in optical response functions are detailed in Refs. 20 and 22 and will not be repeated. [Equation (A6) of Ref. 22 can be directly applied to obtain terms such as  $\hat{\mathbf{i}} \cdot \nabla_{\mathbf{k}} \hat{H}_{\mathbf{k}}$ . Terms such as  $\hat{\mathbf{i}} \cdot \nabla_{\mathbf{k}} (\hat{\mathbf{j}} \cdot \nabla_{\mathbf{k}} \hat{H}_{\mathbf{k}})$  can be obtained from Eq. (A22) of Ref. 22 by first choosing  $\hat{\mathbf{q}} = \hat{\mathbf{i}} + \hat{\mathbf{j}}$  and then subtracting the terms obtained with  $\hat{\mathbf{q}} = \hat{\mathbf{i}}$  and  $\hat{\mathbf{q}} = \hat{\mathbf{j}}$ .] We only present the final expression for the optical activity tensor  $\eta_{ijl}$  here.

Let  $G^{c,L}$  be the LDA conduction-band Green function,  $H_i = \hat{\mathbf{i}} \cdot \nabla_{\mathbf{k}} \hat{H}_{\mathbf{k}}^L$  and  $H_{ij} = \hat{\mathbf{i}} \cdot \nabla_{\mathbf{k}} (\hat{\mathbf{j}} \cdot \nabla_{\mathbf{k}} \hat{H}_{\mathbf{k}}^L)$ . Also define

$$\begin{aligned} \xi_{jil} &= \Delta \langle n\mathbf{k} | H_j | m\mathbf{k} \rangle \\ &\quad \times \langle m\mathbf{k} | H_i (G_{m\mathbf{k}}^{c,L})^2 G_{m\mathbf{k}}^c(\omega) G_{m\mathbf{k}}^c(-\omega) G_{n\mathbf{k}}^{c,L} H_l | n\mathbf{k} \rangle. \end{aligned} \quad (\text{B2})$$

The  $vvc$  term can be written as

$$\begin{aligned} \eta_{ijk}^{vvc}(\omega) &= 4\pi\bar{\Omega}_0 \int_{\text{BZ}} d\mathbf{k} \sum_{n,m}^v \text{Im} \{ 2 \langle n\mathbf{k} | H_j | m\mathbf{k} \rangle \langle m\mathbf{k} | H_i G_{m\mathbf{k}}^{c,L} G_{m\mathbf{k}}^c(\omega) G_{m\mathbf{k}}^c(-\omega) \\ &\quad \times [\omega^2 - (\epsilon_{m\mathbf{k}} - \hat{H}_{\mathbf{k}})^2 - (\epsilon_{n\mathbf{k}} - \hat{H}_{\mathbf{k}})^2 - (\epsilon_{m\mathbf{k}} - \hat{H}_{\mathbf{k}})(\epsilon_{n\mathbf{k}} - \hat{H}_{\mathbf{k}})] \\ &\quad \times G_{n\mathbf{k}}^{c,L} G_{n\mathbf{k}}^c(\omega) G_{n\mathbf{k}}^c(-\omega) H_l | n\mathbf{k} \rangle - \xi_{jli} - \xi_{ilj} + \xi_{jil} + \xi_{ijl} \}. \end{aligned} \quad (\text{B3})$$

Defining

$$\xi_{jil}^{(1)} = \langle n\mathbf{k} | H_j G_{n\mathbf{k}}^{c,L} H_i G_{n\mathbf{k}}^{c,L} G_{n\mathbf{k}}^c(\omega) G_{n\mathbf{k}}^c(-\omega) H_l | n\mathbf{k} \rangle \quad (\text{B4})$$

and

$$\xi_{jil}^{(2)} = \Delta \langle n\mathbf{k} | H_j G_{n\mathbf{k}}^{c,L} H_i (G_{n\mathbf{k}}^{c,L})^2 G_{n\mathbf{k}}^c(\omega) G_{n\mathbf{k}}^c(-\omega) H_l | n\mathbf{k} \rangle, \quad (\text{B5})$$

the  $ccv$  term is

$$\eta_{ijl}^{ccv}(\omega) = 4\pi\bar{\Omega}_0 \int_{\text{BZ}} d\mathbf{k} \sum_n^v \text{Im} \{ -\xi_{jli}^{(1)} + \xi_{jil}^{(1)} - \xi_{jil}^{(2)} - \xi_{ijl}^{(2)} + \xi_{jli}^{(2)} + \xi_{lji}^{(2)} \}. \quad (\text{B6})$$

In Eqs. (B3) and (B6), the additional  $\xi$  and  $\xi^{(2)}$  terms are due to the velocity normalization of  $\hat{\mathbf{i}} \cdot \nabla_{\mathbf{k}} (\hat{\mathbf{j}} \cdot \nabla_{\mathbf{k}} \hat{H}_{\mathbf{k}})$  and  $\hat{\mathbf{j}} \cdot \nabla_{\mathbf{k}} (\hat{\mathbf{l}} \cdot \nabla_{\mathbf{k}} \hat{H}_{\mathbf{k}})$ . The  $cv$  term is

$$\eta_{ijl}^{cv}(\omega) = 4\pi\bar{\Omega}_0 \int_{\text{BZ}} d\mathbf{k} \sum_n^v \text{Im} \{ -\langle n\mathbf{k} | H_l (G_{n\mathbf{k}}^{cL})^2 (\epsilon_{n\mathbf{k}} - \hat{H}_{\mathbf{k}}) G_{n\mathbf{k}}^c(\omega) G_{n\mathbf{k}}^c(-\omega) H_{ij} | n\mathbf{k} \rangle + \langle n\mathbf{k} | H_l (G_{n\mathbf{k}}^{cL})^2 (\epsilon_{n\mathbf{k}} - \hat{H}_{\mathbf{k}}) G_{n\mathbf{k}}^c(\omega) G_{n\mathbf{k}}(-\omega) H_{jl} | n\mathbf{k} \rangle \}. \quad (\text{B7})$$

\*Present address: Department of Physics, University of California, Davis, CA 95616.

<sup>1</sup>H. Zhong, Z. H. Levine, D. C. Allan, and J. W. Wilkins, *Phys. Rev. Lett.* **69**, 379 (1992); **70**, 1032(E) (1993). In the paper, the third term in Eq. (1) should be  $(i/4\pi)\eta_{ijl}q_jE_l$  instead of  $i\eta_{ijl}q_jE_l$ ; Eq. (2) should be  $\rho = \frac{1}{2}\alpha\omega(n_+ - n_-) = \frac{1}{2}\alpha^2\omega^2\eta_{231}$ .

<sup>2</sup>T. M. Lowry, *Optical Rotatory Power* (Dover, New York, 1964), p. 7.

<sup>3</sup>M. F. Brulard, *J. Phys. (Paris) Ser. III* **2**, 393 (1893), and references therein.

<sup>4</sup>J. Jerphagnon and D. S. Chemla, *J. Chem. Phys.* **65**, 1522 (1976).

<sup>5</sup>A. M. Glazer and K. Stadnicka, *J. Appl. Crystallogr.* **19**, 108 (1986).

<sup>6</sup>E. U. Condon, *Rev. Mod. Phys.* **9**, 432 (1937).

<sup>7</sup>E. U. Condon, W. Altar, and H. Eyring, *J. Chem. Phys.* **5**, 753 (1937).

<sup>8</sup>T. M. Lowry, *Optical Rotatory Power* (Ref. 2), p. 392.

<sup>9</sup>S. Chandrasekhar, *Proc. Indian Acad. Sci. Sect. A* **37**, 468 (1953). The coupled-oscillator model considers one atom (or molecule) to be a linear oscillator with a given orientation weakly coupled to the oscillator associated with the next atom (or molecule) along the helix; the orientation of this second oscillator is rotated with respect to the first by the rotation of the helix. The three model parameters (frequency and orientation of the oscillator and the weak coupling which splits the frequencies) are as follows: (i) The frequency is adjusted to reproduce of  $2n_o + n_e$  at zero frequency, (ii) the orientation is adjusted to get the correct extraordinary dielectric constant ( $n_e$ ), and (iii) the weak coupling is adjusted to produce the coefficient  $k$  in Eq. (1.2).

<sup>10</sup>S. H. Wemple and M. DiDomenico, Jr., *Phys. Rev. B* **3**, 1338 (1971).

<sup>11</sup>M. Born and E. Wolf, *Principles of Optics*, 6th ed. (Pergamon, New York, 1989), p. 97; J. N. Hodgson, *Optical Absorption and Dispersion in Solids* (Chapman and Hall, London, 1970), p. 17.

<sup>12</sup>V. Devarajan and A. M. Glazer, *Acta Crystallogr. Sec. A* **42**, 560 (1986).

<sup>13</sup>S. Baroni, P. Giannozzi, and A. Testa, *Phys. Rev. Lett.* **58**, 1861 (1987).

<sup>14</sup>M. S. Hybertsen and S. G. Louie, *Phys. Rev. B* **34**, 5390 (1986).

<sup>15</sup>M. S. Hybertsen and S. G. Louie, *Phys. Rev. B* **35**, 5585 (1987).

<sup>16</sup>S. de Gironcoli, S. Baroni, and R. Resta, *Phys. Rev. Lett.* **62**, 2853 (1989).

<sup>17</sup>M. Alouani, L. Brey, and N. E. Christensen, *Phys. Rev. B* **37**, 1167 (1988).

<sup>18</sup>Y. Xu and W. Y. Ching, *Phys. Rev. B* **44**, 11048 (1991), and references therein; Table I,  $\alpha$ -quartz  $\epsilon_o$  and  $\epsilon_e$ , private communication. (The average was published in the reference.)

<sup>19</sup>Z. H. Levine and D. C. Allan, *Phys. Rev. Lett.* **63**, 1719 (1989).

<sup>20</sup>Z. H. Levine and D. C. Allan, *Phys. Rev. B* **43**, 4187 (1991).

<sup>21</sup>Z. H. Levine and D. C. Allan, *Phys. Rev. Lett.* **66**, 41 (1991).

<sup>22</sup>Z. H. Levine and D. C. Allan, *Phys. Rev. B* **44**, 12781 (1991).

<sup>23</sup>Z. H. Levine, H. Zhong, S. Wei, D. C. Allan, and J. W. Wilkins, *Phys. Rev. B* **45**, 4131 (1992).

<sup>24</sup>H. Zhong, Ph.D. thesis, Ohio State University, 1993.

<sup>25</sup>L. D. Landau and E. M. Lifschitz, *Electrodynamics of Continuous Media* (Pergamon, Oxford, 1957), pp. 337–343. Our  $\eta$  is  $\gamma$  in this reference; our  $g_{ij}$  is  $g_{ij}$  in this reference times the refractive index.

<sup>26</sup>A. Yariv and P. Yeh, *Optical Waves in Crystals* (Wiley, New York, 1984), p. 94.

<sup>27</sup>J. F. Nye, *Physical Properties of Crystals* (Clarendon, Oxford, 1989), p. 249.

<sup>28</sup>J. Kobayashi, T. Takahashi, T. Hosokawa, and Y. Uesu, *J. Appl. Phys.* **49**, 809 (1978).

<sup>29</sup>J. K. O'Loane, *Chem. Rev.* **80**, 41 (1980).

<sup>30</sup>H. Futama and R. Pepinsky, *J. Phys. Soc. Jpn.* **17**, 725 (1962).

<sup>31</sup>M. V. Hobden, *Acta Crystallogr. Sec. A* **24**, 676 (1968).

<sup>32</sup>A. F. Konstantinova, N. R. Ivanov, and B. N. Grechushnikov, *Kristallografiya* **14**, 283 (1969) [*Sov. Phys. Crystallogr.* **14**, 222 (1969)].

<sup>33</sup>P. Etchegoin and M. Cardona, *Solid State Commun.* **82**, 655 (1992).

<sup>34</sup>A. Zangwill and P. Soven, *Phys. Rev. A* **21**, 1561 (1980).

<sup>35</sup>R. O. Jones and O. Gunnarsson, *Rev. Mod. Phys.* **61**, 689 (1989).

<sup>36</sup>L. Hedin, *Phys. Rev.* **139**, A796 (1965); L. Hedin and S. Lundqvist, in *Solid State Physics*, edited by H. Ehrenreich, F. Seitz, and D. Turnbull (Academic, New York, 1969), Vol. 23, p. 1.

<sup>37</sup>R. W. Godby, M. Schlüter, and L. J. Sham, *Phys. Rev. B* **37**, 10159 (1988).

<sup>38</sup>V. Ambegaokar and W. Kohn, *Phys. Rev.* **117**, 423 (1960).

<sup>39</sup>G. Baym, *Lectures on Quantum Mechanics* (Benjamin/Cummings, Menlo Park, CA, 1973), p. 267.

<sup>40</sup>D. R. Hamann, *Phys. Rev. B* **40**, 2980 (1989).

<sup>41</sup>S. L. Adler, *Phys. Rev.* **126**, 413 (1962).

<sup>42</sup>N. Wiser, *Phys. Rev.* **129**, 62 (1963).

<sup>43</sup>C. Kittel, *Quantum Theory of Solids* (Wiley, New York, 1963), p. 183.

<sup>44</sup>D. E. Aspnes, *Phys. Rev. B* **6**, 4648 (1972).

<sup>45</sup>M. P. Teter, M. C. Payne, and D. C. Allan, *Phys. Rev. B* **40**, 12255 (1989).

- <sup>46</sup>L. Kleinman and D. M. Bylander, *Phys. Rev. Lett.* **48**, 1425 (1982).
- <sup>47</sup>M. P. Teter (private communication). This is a Padé approximant to the data of Ceperley and Alder, which therefore has continuous derivatives unlike the Perdew-Zunger parametrization.
- <sup>48</sup>P. E. Blöchl, *Phys. Rev. B* **41**, 5414 (1990); D. Vanderbilt, *ibid.* **41**, 7892 (1990).
- <sup>49</sup>E. L. Shirley, D. C. Allan, R. M. Martin, and J. D. Joannopoulos, *Phys. Rev. B* **40**, 3652 (1989).
- <sup>50</sup>W. Henrion and F. Eckart, *Z. Naturforsch. A* **19**, 1024 (1964).
- <sup>51</sup>X. Gonze, D. C. Allan, and M. P. Teter, *Phys. Rev. Lett.* **68**, 3603 (1992).
- <sup>52</sup>L. Levien, C. T. Prewitt, and D. Weidner, *Am. Mineral.* **65**, 920 (1980).
- <sup>53</sup>S. Tutihasi and I. Chen, *Phys. Rev.* **158**, 623 (1967).
- <sup>54</sup>The same set, with six points in  $\frac{1}{12}$  of the Brillouin zone, was used in Ref. 51.
- <sup>55</sup>E. J. Danielewicz and P. D. Coleman, *Appl. Opt.* **13**, 1164 (1974).
- <sup>56</sup>A. Carvalho, *C. R. Acad. Sci.* **126**, 728 (1898); cited in D. E. Gray, *American Institute of Physics Handbook*, 2nd ed. (McGraw-Hill, New York, 1963), pp. 6–26.
- <sup>57</sup>F. F. Martens, *Ann. Phys. (Leipzig)* **6**, 603 (1901); cited in D. E. Gray, *American Institute of Physics Handbook* (Ref. 56).
- <sup>58</sup>F. Gervais and B. Piriou, *Phys. Rev. B* **11**, 3944 (1975); see Eq. (2).
- <sup>59</sup>Z. H. Levine, *Phys. Rev. B* **42**, 3567 (1990); **44**, 5981(E) (1991).
- <sup>60</sup>G. H. Sherman and P. D. Coleman, *J. Appl. Phys.* **44**, 238 (1973).
- <sup>61</sup>B. F. Levine, *Phys. Rev. B* **7**, 2600 (1973).
- <sup>62</sup>S. Baroni and R. Resta, *Phys. Rev. B* **33**, 7017 (1986).
- <sup>63</sup>J. E. Adams and W. Haas, in *The Physics of Selenium and Tellurium*, edited by W. C. Cooper (Permagon, New York, 1969), p. 293.
- <sup>64</sup>G. W. Day, *Appl. Phys. Lett.* **18**, 347 (1971).
- <sup>65</sup>G. Szivessy and C. Münster, *Ann. Phys. (Leipzig)* **20**, 703 (1934).
- <sup>66</sup>R. Claus, *Phys. Status Solidi B* **96**, 545 (1979).
- <sup>67</sup>S. S. Kotsur and I. V. Stasyuk, *Phys. Status Solidi B* **149**, 347 (1988).
- <sup>68</sup>W. Voigt, *Ann. Phys. (Leipzig)* **18**, 645 (1905).
- <sup>69</sup>F. Wever, *Jahrb. Philos. Fak. Univ. Göttingen* **2**, 206 (1920).
- <sup>70</sup>G. Szivessy and C. Schweers, *Ann. Phys.* **1**, 891 (1929).
- <sup>71</sup>G. Bruhat and P. Grivet, *J. Phys. Radium* **6**, 12 (1935).
- <sup>72</sup>E. D. Palik, *Handbook of Optical Constants of Solids II* (Academic, Orlando, 1985), p. 691.
- <sup>73</sup>J. Jerphagnon, E. Batifol, and M. Sourbe, *C. R. Acad. Sci. Paris Ser. B* **265**, 400 (1967).
- <sup>74</sup>C. K. N. Patel, *Phys. Rev. B* **16**, 613 (1966).
- <sup>75</sup>B. F. Levine and C. G. Bethea, *Appl. Phys. Lett.* **20**, 272 (1972).
- <sup>76</sup>R. C. Miller and A. Savage, *Phys. Rev.* **128**, 2175 (1962).
- <sup>77</sup>J. Jerphagnon and S. K. Kurtz, *Phys. Rev. B* **1**, 1738 (1970).
- <sup>78</sup>The nonlocal potential discussed here is independent of the wave function  $\psi$ . The nonlocal Hartree-Fock potential is gauge invariant since the potential itself is a function of the wave function. Nonlocal potentials which depend on the wave function, such as the Hartree-Fock potential, are not discussed here. See D. H. Kobe, *Phys. Rev. A* **19**, 205 (1979).
- <sup>79</sup>See G. Baym, *Lectures on Quantum Mechanics* (Ref. 39), p. 137.
- <sup>80</sup>A. M. Korolev, *Yad. Fiz.* **6**, 353 (1966) [*Sov. J. Nucl. Phys.* **6**, 257 (1967)].